DYNAMIC STRENGTH OF PORCINE ARTERIES

A Thesis
Presented to
The Academic Faculty

By

Jinwu Fan

In Partial Fulfillment
Of the Requirements for the Degree
Master of Science in the
School of Mechanical Engineering

Georgia Institute of Technology

December 2007

DYNAMIC STRENGTH OF PORCINE ARTERIES

Approved by:

Dr. David Ku, Advisor
School of Mechanical Engineering
Georgia Institute of Technology

Dr. Steve Johnson
School of Mechanical Engineering
Georgia Institute of Technology

Dr. Alexanda Rachev
School of Mechanical Engineering
Georgia Institute of Technology

Date Approved:

ACKNOWLEDGMENTS

Thank you Mom, Dad and my wife for all of your support, love and encouragement.

Dr. Ku, thank you for your direction, encouragement and words of wisdom. Thank you for doing everything that you could do to make my research successful. I would also like to thank Dr. Johnson for your direction and help, Dr. Rachev for your patience and your constant willingness to help. To Dr. Y's lab and Dr. Vito's lab thank you for driving me to slaughter house and using the clinic tools. Dr. Guldberg and lab, thank you for letting me do my testing. Angela and Srin thank you for your help. Dr. Gleason's Lab, thank you William and Julia for your help. I would like to thank my lab mates, LauraLee, Ruhul, Dave, Andrea and Jason, you made me my time here run smoothly. I couldn't have asked for better friends.

To all my friends who have become family here in Atlanta. Thank you for everything and I have spent a great time here.

TABLE OF CONTENTS

Page

LIST OF TABLES

Page

LIST OF FIGURES

Page

SUMMARY

The ultimate strength of collagenous blood vessels is important for clinical problems of trauma and plaque rupture. Cyclic tests require high frequencies that may affect the strength properties of the soft tissue. Experimental results of mechanical response of blood vessels to physiologic loads can be used to model and predict plaque rupture and direct medical therapy or surgical intervention.

The goal of the study is to measure the mechanical failure properties of arteries to determine if they are strain rate and cycle dependant and to measure the progressive damage of arteries with time dependent loading.

Ring specimens of porcine carotid arteries were preconditioned and then pulled to failure. In all cases, the intima broke first. Ultimate strength increased as a weak function of increasing strain rates. The ultimate strength at 100 mm/s was 4.54 MPa, greater than the 3.26 MPa at 0.1 mm/s. Strain rates between 1 and 100 mm/s correspond to a cyclic frequency of 0.5 Hz to 5 Hz for fatigue testing. In contrast, ultimate strain in arteries was independence of strain rate over the range tested.

The testing results showed that there were no significant differences on stress and strain among fresh arteries and arteries stored at 5° C for one week and two weeks.

The values of ultimate strength showed a 35% increase after 10,000 cycling loading, nonetheless, the ultimate strain had a 13% decrease after cycling and the difference was statistically significant with $p=0.018$.

The creep tests showed a logarithmic relationship between stress magnitude and stress duration for this soft tissue. The creep testing indicates that damage is

accumulating and the negative slope of the time vs. load curve indicates that the material will fail faster when increase the testing loads.

All the test results may be useful for developing a mathematical model to predict the behavior of arterial soft tissues and may be extended to estimate fracture and fatigue in the atherosclerotic plaque cap.

CHAPTER 1

INTRODUCTION

The dominant pattern of arteriosclerosis is atherosclerosis, which is the No. 1 cause of death in the United States and is a major cause of disability. In 1996, it caused almost 1 million deaths which were twice as many as cancer caused and 10 times as many as accidents caused [1]. Atherosclerosis is a form of arteriosclerosis characterized by the deposition of atheromatous plaques containing cholesterol and lipids on the innermost layer of the walls of large and medium-sized arteries in which the wall of an artery becomes thicker and less elastic.

One currently favored theory is that called response-to-injury hypothesis which suggests that atherosclerosis develops as a result of repetitive injury to the inner lining of the artery. At the very beginning, hypertension, hyperlipidemia, hemodynamic factors and other factors will cause chronic endothelium injury with resulting increased endothelial permeability or dysfunction which increases the accumulation of lipoprotein in the arterial wall. Then smooth muscles emigrate from media to intima and macrophage activate. Smooth muscle cells proliferate in the intima and extracellular matrix forms, and finally the lesion becomes a plaque formation (Kumar[2], Duguid[3]).

The lumen of the arteries narrows as the atheromatous plaques grow. With time, calcium accumulates in the atheromas which may become brittle and rupture. The lumen of the arteries narrows even more with the blood enters a ruptured atheroma which makes it larger. A ruptured atheroma also may spill its fatty contents into the bloodstream which may block an artery elsewhere in the body. More often, the rupture of an atheroma

triggers the formation of platelet-rich thrombus and ultimately leads to occlusion, which is the main cause of a heart attack or stroke. The thrombi due to clot further narrow or even block the artery (Lee [4], Richardson [5]).

The phenomena of plaque cap rupture attributes to two critical causes: one is that an imbalance between the stress imposed on the plaque cap and the innate strength of the cap tissue which leads crack propagation. McCord [6]found that cyclic bending of artery can induce plaque cap fatigue. It was found that rupture of the vasa vasorum and neovascularization could cause plaque cap rupture (Barger [7]). Vasospasm could lead to plaque rupture by exerting a compressing force on the vessels. Narrowed coronary lumina due to plaque and spasm, could also lead to heart attacks and subsequent sudden death (Leary [8]). The plaques altering the distribution of circumferential tensile stress across the intima and high circumferential stress was found to tear the intima (Richardson [9]). Hemodynamic shear stress and turbulence could also trigger the plaque rupture (Gertz [10], Loree [11]). It proposed that mechanical fatigue due to pulsatile cardiovascular pressure environment could cause plaque cap rupture, hypertension led to even worse situation (Bank[12]; Versluis[13]). On the other hand, the increased expression of matrix metalloproteinases (MMP) leads to weakened tissue (Lee [14]). Loss of smooth-muscle cells due to apoptosis may be an important element in the weakening of connective tissue framework of the plaque's fibrous cap (Libby [15]).

Atherosclerosis is a complicated disease, although these mechanisms predominantly describe the acute final rupture, there still a lot work to do, such as finding out a unifying or consistent explanation for this biomechanical process. Although there are disputations on the critical cause of plaque cap rupture, biomechanics contribute a lot

to these diseases. We can use a model to predict the mechanical response of such kind of soft tissues.

Understanding the failure behavior of material is important in describing the material. In general, the fatigue is the process of damage accumulation in a material that is subject to cyclic loading (Suresh [16]), the definition can also apply to metallic composites (Dvorak [17]). The process of fatigue failure of metals due to their crystals slipping past one another in irreversible ways forming cracks which initiate and propagate until the material finally fails. Fatigue failure always happened at the stress condition far below the "safe" stress. Description of fatigue failure requires an understanding of elasticity and plasticity theories. When materials undergo elastic deformation, the stress and strain can be related by Hooke's law, elastic deformation is reversible deformation which means that when unloading the material can go back to its original point. When the material is loaded beyond the elastic limit, it undergoes permanent plastic deformation which means that the material can not go back to its original point when unloading. The process of strain increment under a constant load is called creep. Cyclic loads acting on metals in association with high temperature cause creep-fatigue. The deformation due to enhanced cavitation and sliding by high temperature becomes prominent, that is, time-dependent rather than cycle-dependent (Suresh [16]). The blood vessels with extracellular matrix of plaques could be proposed as a soft composites which is embedded with collagen and glycosaminoglycans (Richardson [5]). So it is feasible to model such soft tissues using the methods that were developed to analysis composites.

Several researchers have studied the mechanical properties of arteries, skin,

sclera, tendons and synthetic materials. Mohan [18] found that the ultimate strength for human mid-thoracic aortas changed from 1.72±0.89MPa for quasi-static tests to 5.07±3.29MPa for dynamic tests. Raghavan [19] showed that ultimate stress for human abdominal aortic aneurysm (AAA) varied from 0.336MPa to 2.351MPa under a strain rate of 30%/min. Johnson [20] found the ultimate strength of human patellar tendon were 64.7 $\pm$ 15.0 MPa and 53.6 $\pm$ 10 MPa for the younger and older group respectively. Edwards [21] measured the tensile properties and found that the tensile strength of skin ranges from 5 to 30 MPa, with the mean showing a maximum of about 21MPa at 8 years, declining to about 17 MPa at 95 years. Ku [22] created a biocompatible material called PVA cryogel that has a mechanical strength between 0.5 MPa and 75 MPa.

The structural components of plaque caps are similar as artery, both are collagen and elastin components. Therefore, knowledge of the mechanical properties of blood vessels, especially arteries, is fundamental to understanding plaque cap rupture. Experimental results of mechanical response of blood vessels to physiologic loads can be used to model and predict plaque rupture and direct medical therapy or surgical intervention.

One of the big impediments to understanding vascular mechanics is the lack of sufficient experimental data. Moreover, the lack of sources restricts the amount of primary data regarding ultimate strength, strain, frequency dependence, and harvest time dependence. Nonetheless, the mechanics surrounding plaque cap rupture demand measurements of all these parameters.

Much work has been done to determine the static and dynamic mechanical properties of arteries, most of them, however, focused on the relationship of stress-strain

or pressure-volume before the arteries rupture (Bergel[23], [24]; Dobrin[25]; Langewouters[26]; Silver[27]).

Elastic response and the ultimate strength are the two important mechanical properties in consideration of plaque cap rupture. The ultimate strength of blood vessels is important for clinical problems of trauma and plaque rupture. Trauma related to motor vehicle accidents can create strain rates of 100 mm/s. cyclic fatigue tests may also require high frequencies and strain rate that may affect the strength properties of the soft tissue. The yield points and ultimate strengths depend on the unfolding of collagen molecules, collagen crosslinks, and the fiber-matrix bonding this composite structure. Fibers were uncrumped and straightened in the necrotic region and caused the increased stiffness of the aorta that is similar to the stress response of normal artery (Angouras[28]). The non-linear behavior of animal soft tissues makes the determination of a plastic yield point difficult to distinguish.

Background

Artery Structure

The mechanical properties of a material depend on its composition, structure, and environment, the arterial wall exhibits a wide range of behaviors depending on the location in the body. The principal organized constituents of the arterial wall are the smooth muscle cells and the extracellular matrix, composed of elastin, collagen, and ground substance. Smooth muscle cells in most vessels tend to be oriented helically, almost circumferentially. The extracellular matrix gives the arterial tissue its strength and basic shape as elastin and collagen are arranged into reinforcement structures.

All arteries are made of three concentric layers: the innermost layer is the intima, consists of one layer of endothelial cells held on a basal lamina. The normal intima has negligible mechanical properties because it is very thin although intimal hyperplasia or other extreme conditions may affect the arteries properties. The middle layer is called the media, consists mostly of elastic fibers and smooth muscle cells. It contributes greatly to mechanical response of arteries. The outermost layer is adventitia, a dense network of collagen fibers interspersed with fibroblasts, elastic fibers, nerves, and vasa vasorum.

Artery Mechanics

In vivo, noninvasive technologies, such as cineangiography, intravascular ultrasound, echography, and magnetic resonance imaging, can do some job on establishing the behavior of arteries (Bank[29]). Most attempts focused on in vitro evaluation of the mechanical response of arteries. A uniaxial tensile test on arterial strips or rings is the easiest way to study the mechanical response of excised tissues and to obtain stress-strain curves. This approach has been done by a lot of people and followed

widely in the literature for different soft tissues (Fung [30], Monson [31], Bergel[23], Lawton[32], Mohan [18]). Biaxial tests, pressurization tests and cyclic tests also have been reported in the literature (Mohan[33], Sipkema [34]).

Mechanical Model

There are a lot of mechanical models for soft tissue with a lot of assumptions been made. The artery is subjected to internal pressure and axial extension. It is always assumed to be a straight circular cylinder that is symmetric. Thin-walled cylinder theory has been used to model the mechanical response of arteries, such as buckling (Han [35]). To determine the intramural distribution of stress and strain, more refined thick-walled theory has been used without considering the actual heterogeneity and the different layers properties of arteries (Sato [36]). For simplicity, the artery sometimes is assumed to have homogenized properties through the whole wall. Due to its special structure, artery mechanical response exhibits repeatable hyperelastic behavior after preconditioning, thus, many mathematical model used strain energy function (Fung [30]). Plus, incompressibility is frequently used to build the artery model.

No matter what kind of model, it needs several material properties, such as material constants, modulus, strain, etc. All these parameters can only be obtained by experiments.

It is possible to use finite element method to analysis the mechanical response of arteries. Linear and nonlinear material models have been proposed. The big advantage of this method is that it can solve the equations without analytic solutions; moreover, it potentially can discover and mimic the mechanical response of branches, aneurysms, plaque cap rupture, and stenoses (Blondel [37], Hayashi[38], Richardson [5], Tang [39,

40], Wootton [41]). However, the implementation of realistic material properties for arterial tissues is still under development and improper simplifying can lead to problems.

Hypothesis

The plaque cap of an atheroma, a biological composite soft tissue, exhibits mechanical fatigue leading to a local weak point that can rupture. Cyclic pressure and local stress concentration can cause the plaque cap to rupture and eventually the formation or presence of a thrombus. The hypotheses of this work are that:

1. Arteries exhibit an ultimate strength that is strain rate dependent.
2. Arteries exhibit progressive damage above a threshold stress level that is less than the ultimate stress.
3. Polymeric vascular graft can be made which exhibit physiology compliance.

Specific Aims

The goal of this work is to determine the mechanical behavior of porcine coronary arteries. Specifically, the aims are to:

1. Quantify the ultimate strength and strain for arterial soft tissues. Define the range of biological variability and establish statistical norms.
2. Compare the ultimate strength of arteries with 10,000 cyclic loading under displacement control to the artery samples without cyclic loading.

3. Measure ultimate stress-creep time creep properties of porcine carotid arteries and find the critical creep loading point.
4. Measure and compare the ultiamte strength and strain of porcine arteries that are fresh, one-week, and two-week storaged.
5. Measure and compare pressure-strain mechanical properties of porcine carotid arteries and SaluBridge in the range of physiology pressure.

CHAPTER 2

METHODOLOGY

Ultimate Strength Tests and Creep tests have been performed in this work. Two materials, porcine common carotid harvested from pigs at Hollifield Farms (Covington, GA) and synthetic biocompatible polyner SaluBridge created by SaluMedica (Atlanta, GA), have been used.

Although Ring specimens and dumbbell shape specimens are both one dimensional tests, ring specimens were used because they are easier to obtain from the tubular structure of the arteries. Ring sample can relieve the experimental error comes from the inappropriate clamping dumbbell specimens which can cause the specimens slide or break in the neighborhood of the clamp (Mohan [18]; Raghavan [19]). There are significant damages that could occur from preparing uniaxial dumbbell shaped strips. Dumbbell strips would also be difficult to obtain because of the small diameter of the artery.

Failure of the ring specimen was defined as a complete tear separation of the arterial wall. The final stress at failure represented the ultimate strength for the tension tests. To determine the final stress, an equation was derived based on the assumption of incompressibility [42] which means that the initial volume V_i and final volume V are equal. The derivation is shown in the equations below:

$$V_i = A_i * C_i \tag{1}$$

$$V = A * C \tag{2}$$

Incompressibility: $$V = V_i \quad (3)$$

$$A_i * C_i = A * C \quad (4)$$

$$A = A_i * \frac{C_i}{C} = A_i * \frac{1}{\lambda} \quad (5)$$

Where A_i and A are the initial cross-sectional area and the final cross-sectional area, C_i and C are the initial circumference and the final circumference. In the present experiments the stretch ratio λ is defined as the ratio of the final and initial circumference, Equation (6).

The ultimate stress, σ_{ult} defined by the load at the breaking point of the sample divided by the final cross-sectional area, was calculated using Equation (8). The ultimate stress is a function of the final load and the final cross-sectional area. However, the final cross-sectional area was difficult to measure. The stretch ratio relates the final and initial area with the assumption of incompressibility. That means the final area equals the initial area divided by the stretch ratio. Therefore, the ultimate stress can by calculated by the load at the breaking point of the sample, the stretch ratio and the initial cross-sectional area. The initial cross-sectional area is the product of the initial width of the sample, L_i, and the initial thickness, H_i.

Stretch Ratio: $$\lambda = C / C_i \quad (6)$$

Initial Cross-Section Area: $$A_i = L_i * H_i \quad (7)$$

Ultimate Cauchy Stress: $$\sigma_{ult} = \frac{F_{ult} * \lambda}{A_i} \quad (8)$$

In order to get an estimation of the equivalent pressure in an intact artery the following simplified assumptions were used. It was assumed that a tubular specimen will burst when the circumferential wall stress is equal to the ultimate stress σ_{ult}. However, when an artery is under physiologic load conditions it is in a state of plane strain and ndergoes finite two dimensional stretches. The stretch ratios are:

$$\lambda_\theta = \frac{R}{R_i} \tag{9}$$

$$\lambda_z = \frac{L}{L_i} \tag{10}$$

The wall stress in the circumferential direction of a tubular specimen is calculated by the following equation:

$$\sigma = \frac{PR}{H} \tag{11}$$

Where R and H are the deformed radius and thickness respectively. Due to incompressibility:

$$T = \frac{H_i}{\lambda_\theta \lambda_z} \tag{12}$$

Substituting Equation (9), (10), and (12) into Equation (11) gives the equation:

$$\sigma_\theta = \frac{\lambda_\theta^2 \lambda_z P_i R_i}{H_i} \tag{13}$$

Rewritten to solve for the pressure, P:

$$P = \frac{H_i \sigma_\theta}{\lambda_\theta^2 \lambda_z R_i} \tag{14}$$

This equation can calculate the pressure if we know the initial dimensions, the stress and the stretch ratios. The axial stretch ratio λ_z in situ is on the order of 1.5 which are measured by Chin Quee [43]. He recorded that the ratio between the midwall diameter of the artery at the state of bursting and the diameter at zero pressure is on the order of 1.15 which is the values of λ_θ. From Equation (14) we can estimate the corresponding pressures. Compliance C can be derived from the data. Compliance is a measure of the normalized change in diameter for a pressure rise and expressed as the following:

$$C = \frac{\Delta D}{D_i \Delta P} \tag{15}$$

Where ΔD is the change of diameter, D_i is the initial diameter, and ΔP is the change of diameter.

Ultimate Strength Test

Ring specimens were pulled in tension until they failed. The load at failure was recorded as the ultimate load, and the ultimate stress was calculated. The purpose of these experiments was to quantity ultimate stress and to find the strain rate effects for the failure of porcine common carotid arteries.

Cyclic Test

Ring specimens were cycled for 10,000 cycles with displacement control, and then pulled in tension until failure. The frequency of the cyclic tests was set at 2 Hz because this value is close to physiologic frequency of heart beats (~1.2 Hz) and strain

rates effects testing showed that there are no significant differences with cyclic testing at 1HZ to 5HZ. The purpose of the cyclic tests was to experimentally determine how fatigue affects the ultimate strength of porcine common carotid arteries.

Creep test

A lever testing system was built to determine the creep in the porcine common carotid arteries. Ring specimens were pulled in constant weights until failure. Four different arteries were tested. The weights were recorded as the ultimate load to calculate the stress. The creep time were recorded during the tests.

Storage time effect

To determine how the *ex vivo* storage affects the mechanical properties of the artery, specimens that were fresh, one-week and two weeks in storage with Phosphate Buffered Solution (PBS, pH=7.4$\pm$0.1) in a refrigerator (5° C) were distracted. There were three groups for the test. Each group contained 16 rings and all groups were distracted at the same strain rates using. The load at failure was recorded as the ultimate load, and the ultimate stress was calculated.

Experimental Protocol

Porcine common carotid arteries were harvested from farm pigs at Hollifield Farms (Covington, GA). The pigs are about six months old. The arteries were transported to the laboratory in coolers packed with ice. The arteries were stored in a segmented culture tray filled with Phosphate Buffered Solution (PBS, pH=7.4±0.1) in a refrigerator (5° C). Testing of the arteries began within three hours of harvest. The PBS (Fisher Scientific) was received as a 10x solution and was diluted to 1 X solution using deionized water to reduce the amount of impurities.

Before the ring was cut from the artery an additional trimming of excess connective tissue was performed. In preparation for testing the artery was cut into rings with a width of approximately 4 mm using a razor blade. To cut the artery the ends were clamped to hold the artery still, and it was aligned next to a metric ruler. The rings were stored in a segmented culture tray filled with PBS (Figure 1).

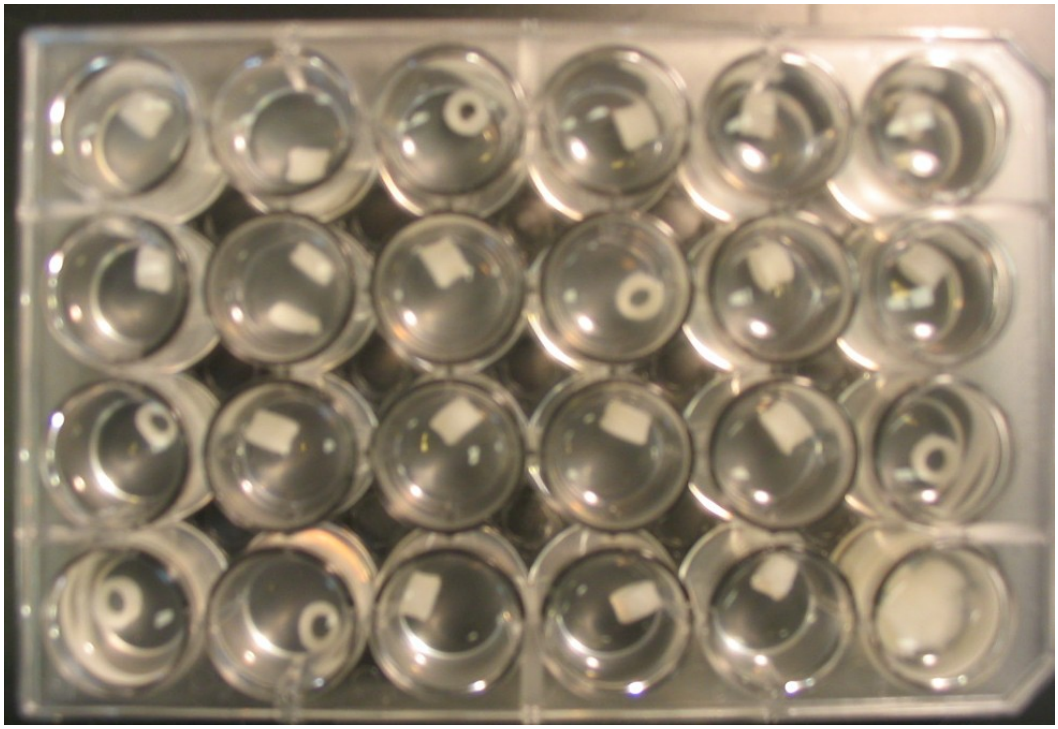

Figure 1: Ring Samples in PBS

The initial inner diameter (D_i), thickness (H_i), and width (L_i) were measured manually for each specimen with digital calipers. A disadvantage to this method of measurement is the possibility that forces applied to the specimen with the calipers caused errors in the measured values. In order to reduce the amount of error, the measurements were taken in triplicate and averaged for use in calculations.

Mechanical Testing

All of the specimens were tested on a servo-controlled electro-mechanical testing machine MTS 858 Mini Bionix (Minneapolis, MN). The 858 Mini Bionix is a universal mechanical testing machine that can be used to test in tension and compression. The 858 Mini Bionix testing system is available in five standard configurations for accurate

testing under axial loads up to ±25 kN with standard displacements of ±50 mm (±2 in). It can run fatigue cycles on biomaterials at frequencies up to 30 Hz. For these tests, the testing machine was fitted with a 100 N load cell. Specimens were hooked at two ends and submerged in the room temperature (20^0C) saline chamber. For the uniaxial test a displacement profile was setup which preconditioned the specimen 25 times at a frequency of 1HZ to 4mm beyond the original ring length, an approximate strain of 40% leading to steady-state behavior. Then the specimens were distracted to ultimate failure at 0.1mm/s, 1mm/s, 10mm/s and 100mm/s. The load, position and time information was collected by the computer software at a rate of 10 data points/sec. The ultimate force was selected as the maximum force measured within 2 seconds of visual breakage. To decrease the experimental error, paired specimens were used.

Once the profile was set, one specimen from the pair was positioned onto two hooks. The hooks were securely placed into the grips of the machine in a position that placed no load on the specimen (Figure 2). The test was started, ran until failure and the final load was recorded as the ultimate load of the material.

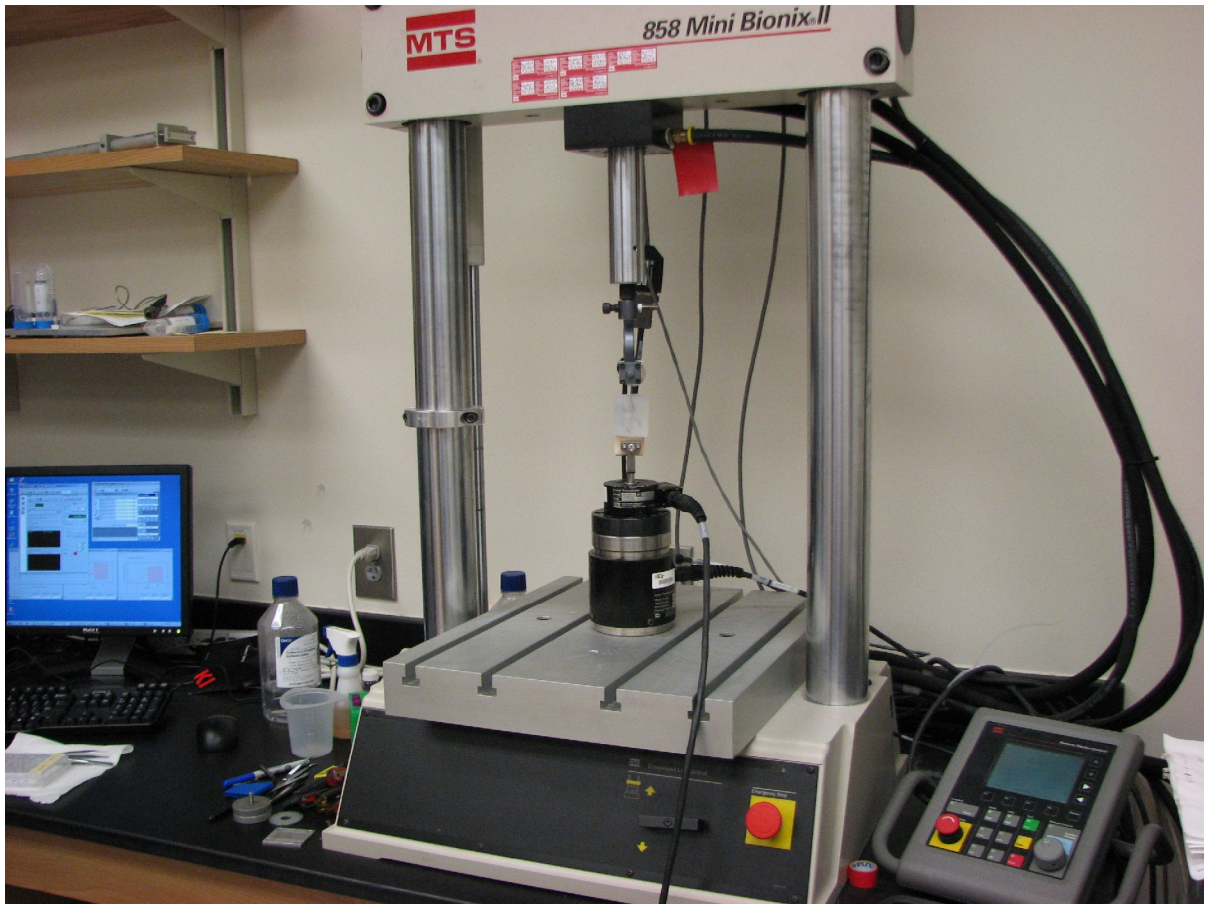

Figure 2: Test Setup

For the cyclic test, a profile was created (Table 1). The artery specimens were preconditioned twenty five cycles to a total displacement of 4 mm beyond the original ring length. To evaluate the effects of cycling, 4 pair specimens were picked up. In each pair, one was tested without cycling, the other was test with 10000 cycling at the frequency of 2 HZ. Each cycling test will last about one and half hour. The specimens

were distracted to ultimate failure at 1mm/s using MTS 858Mini Bionix (Minneapolis, MN). Load, position and time data were recorded by the testing software. The cyclic tests were performed with the specimen totally immersed in a bath of PBS to prevent the tissue from drying. The cyclic tests were also performed at room temperature (20°C).

Table 1: Cyclic Test Profile

Command	Control Rate (mm/s)	Position (mm)	Frequency (HZ)	Number of Cycles
1. Displacement	1	0-2	--	--
2. Amplitude	--	2-4-2-0-2	1	25
3. Displacement	1	2-0	--	--
4. Amplitude	--	0-10-0	2	10000
4. Displacement	1	0-15	1	--

Data Analysis

All of the collected data was imported into Excel and plots of the stress vs. stretch ratio were created. For the tensile tests the plots were used to determine the ultimate stress and ultimate stretch ratio. The final position, L of the test, shown in **Figure 3**, was used to calculate the final circumference of the specimen, C.

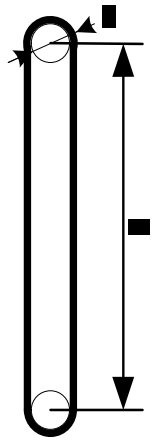

Figure 3: Sample Extended in a Uniaxial Test

$$C = 2 * L + \pi * d \quad (15)$$

The initial circumference, C_i, was calculated as:

$$C_i = \pi * (D_i + H_i) \quad (16)$$

Where D_i and T_i are the initial diameter and thickness of the ring sample separately. The stretch ratios and final stresses were calculated using the equations above. From the collected and calculated data plots were made to determine the effects of the strain rates cycling to ultimate failure.

CHAPTER 3

RESULTS

Ultimate Strength Tests

Four rings were cut along the length of the artery and adjacent rings were paired (Figure 4). The rings were stored in a segmented tray filled with Phosphate Buffered Solution (PBS).

End	A1	A2	A3	A4	A5	A6	B1	B2	B3	B4	B5	B6	C1	C2	C3	C4	End

Figure 4: Representative assignment of one sectioning

Then set the 16 rings into 4 groups:

Groups: A1, A5, B3, C4 tested at 0.1mm/s;

A2, A6, B4, C2 tested at 1mm/s;

A3, B1, B5, C3 tested at 10mm/s;

A4, B2, B6, C4 tested at 100mm/s

Sixty-four rings were tested for ultimate strength. The rings were subjected to a constant rate of displacement and force was measured continuously. The point of failure was defined as a disconnection through the entire wall of the artery ring. This binary endpoint was clear and dramatic. An illustration of this break point is shown in Figure 5. The breaking of the ring structure was complete within 5 frames of the digital video camera which recorded at a speed of 30 frames per second. Thus, the endpoint occurred in a fraction of a second without ambiguity. The location of the break was consistently

away from the hooks, demonstrating that the end-effects were minimal. This separation occurred mostly along the straightened walls of the artery. In all cases, the intimal layer broke first.

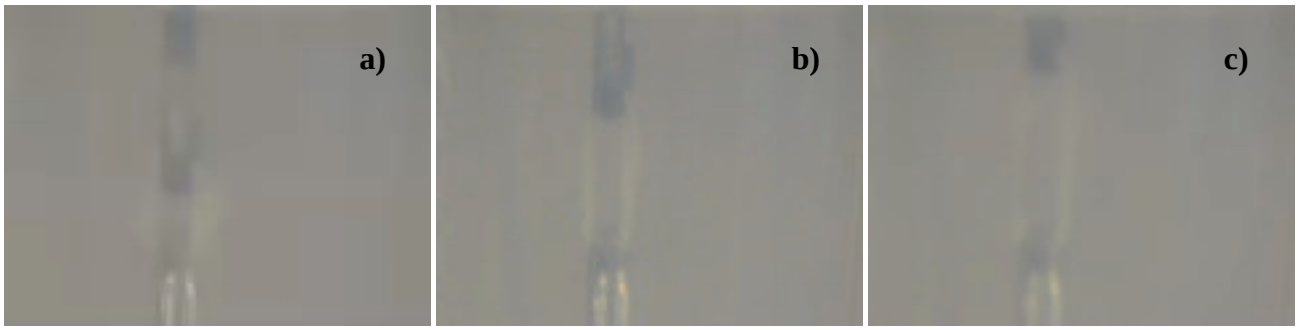

Figure 5: Progression of Artery Failure
a.) Artery placed on the hooks. b.) Artery being pulled. c) Failure of the artery

The number of ring samples cut from each of the arteries and the type of test performed on each is outlined below in the Artery Tables (APPENDIX B). The Average Sample Dimensions are showed in the table below.

Table 2: Sample size (N), initial cross-sectional area (A_i), Length (L_i)(mm), inner diameter (D_i) and wall thickness (H_i) for porcine carotid arteries.

	N	A_i(mm^2)	L_i (mm)	D_i(mm)	H_i(mm)
Artery	64	4.22 (0.54)	4.37 (0.35)	3.58 (0.40)	0.96 (0.09)

For the 64 rings from four arteries, the mean Force of fracture was 11.46 Newton. Since the rings were of a mean thickness of 0.96 mm and a width of 4.37 mm, an initial cross-sectional area is calculated as approximately 4.22 mm^2. Thus, a mean ultimate stress of Force/Area is calculated to be 3.83 MPa. The ultimate strain for these specimens was around 140% of the original length.

The influence of rate of displacement was also investigated. The rate was varied over four orders of magnitude from 0.1 mm/s to 100 mm/s. This range bracketed the estimated physiologic rate of displacement of 1 mm/s expected from a pulsating artery under physiologic pulsatile pressure.

The load and change in position of the grip were recorded directly by the computer for every sample. An example of these plots for the stress vs. strain on artery is shown in figure 6.

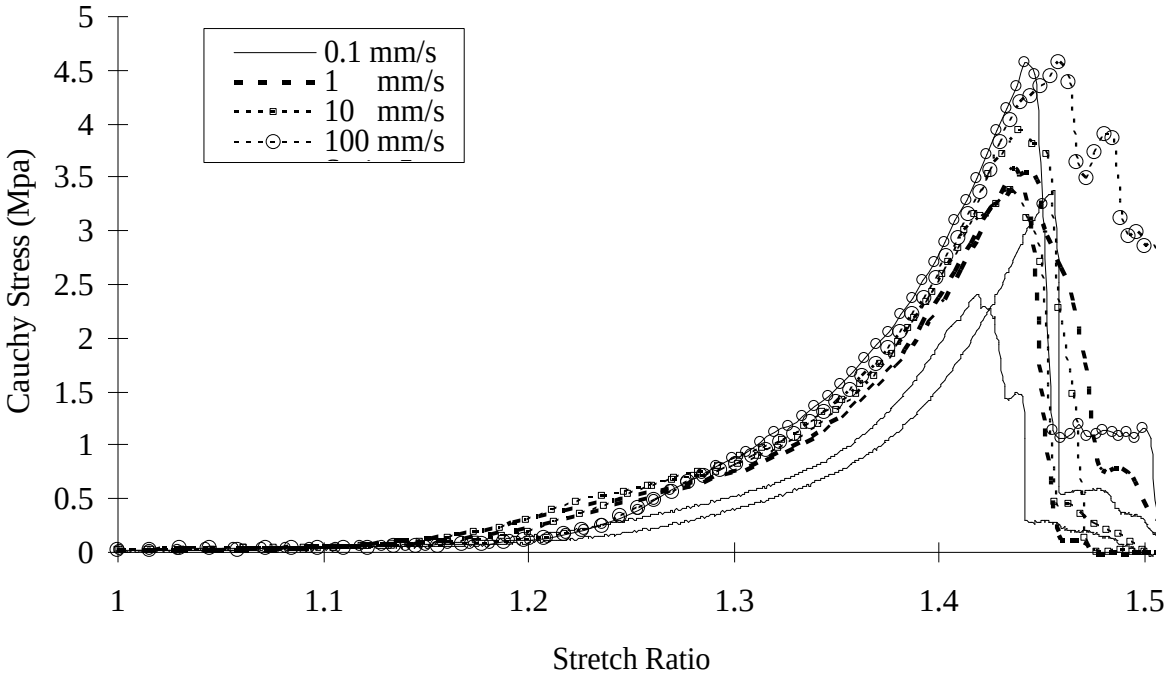

Figure 6: Representative stress-strain response curve at different strain rate

The curves of Cauchy stress vs Time illustrate the strain stiffening behavior of the specimens and the variability in the ultimate stress between specimens. All specimens failed at approximately 1.4 x the original length with little variance. However, the ultimate stress showed some trends with faster speeds giving higher ultimate strengths. Ultimate stress under different strain rate is revealed in Figure 7 and Figure 8. Increasing strain rates resulted in an increased ultimate stress, especially apparent for strain rates from 0.1 mm/s to 100 mm/s. The ultimate stress changed from 3.26±0.67MPa for 0.1mm/s to 4.54±1.00MPa for 100mm/s. The differences between 1mm/s and 10mm/s ($p=0.202$) did not reach statistically significance when we used the Student's paired t-tests method, the level of significance was set at 0.05.

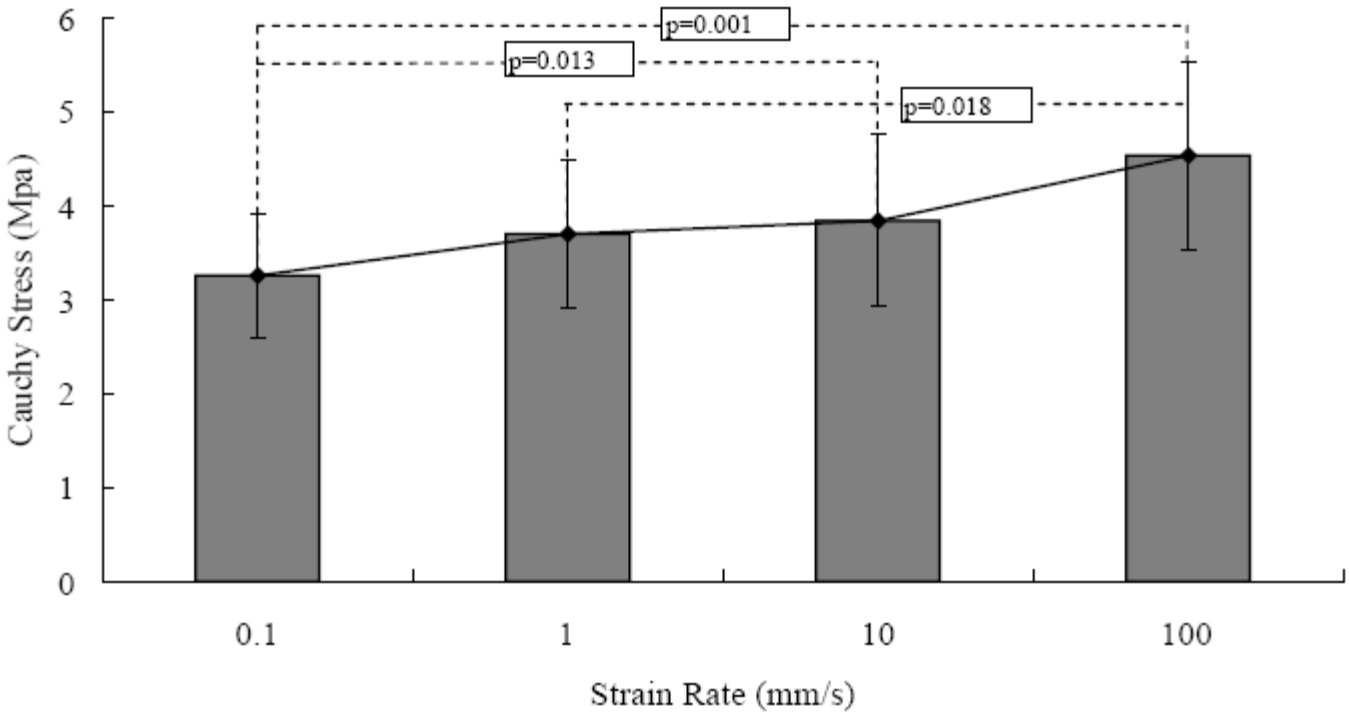

Figure 7. Ultimate Stress under Different Loading Rates. Mean stress ± standard deviation.

From Figure 8, it showed that 70% of the samples failed with a stress range of 3MPa to 5MPa, only 17% of them failed at below 3Mpa. Moreover, no samples failed at below 3MPa for 100mm/s strain rate; no samples failed at below 2.2MPa for all the strain rates. From these studies, one can give a lower bound of ultimate stress for porcine coronary arteries of 2.2 MPa. Using Laplace's Law for cylinders, an equivalent burst pressure would be approximately 3600 mmHg, consistent with the safety factor measured by others. The increased strength at high strain rates would also contribute to a safety margin against burst during impact loading as with trauma.

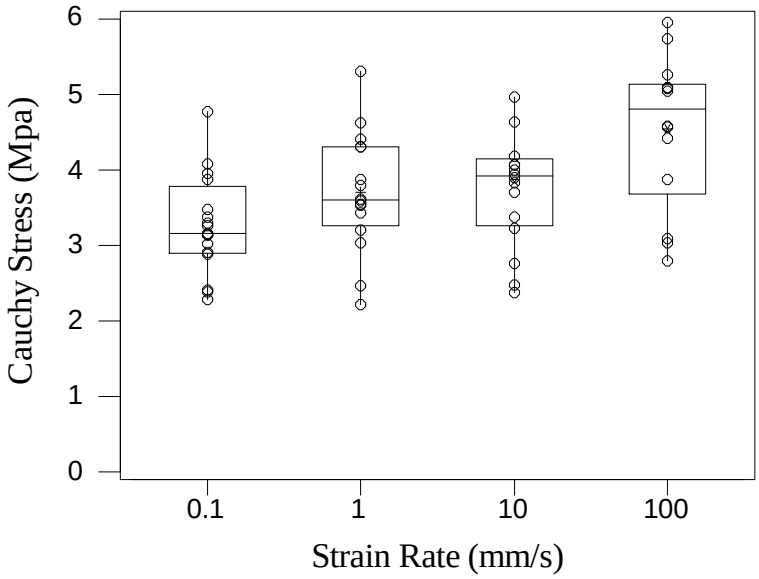

Figure 8. Boxplot of Ultimate Stress under Different Loading Rates

Ultimate strain under different strain rates is revealed in figure 9 and figure 10. The ultimate strain showed less sensitivity to strain rate with a mean value of 1.41. Increasing loading rates did not result in increased ultimate strain. No statistically differences in ultimate strain among those four strain rate were seen when we used the Student's paired t-tests method, the level of significance was set at 0.05.

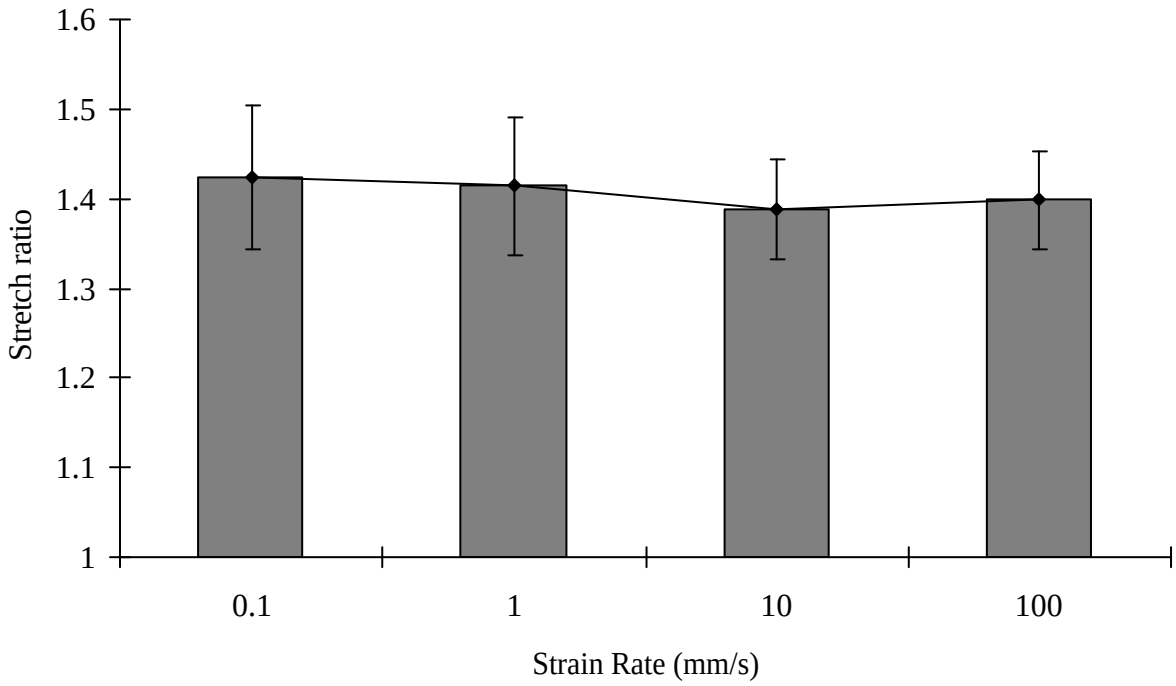

Figure 9. Ultimate Strain under Different Loading Rates. Mean strain ± standard deviation.

It also showed in figure 10 that 90% of the samples failed with a strain range of 1.3 to 1.5, only 5% of them failed at below 1.3 and 5% of them failed at above 1.5. Moreover, no samples failed at below 1.25 and above 1.55.

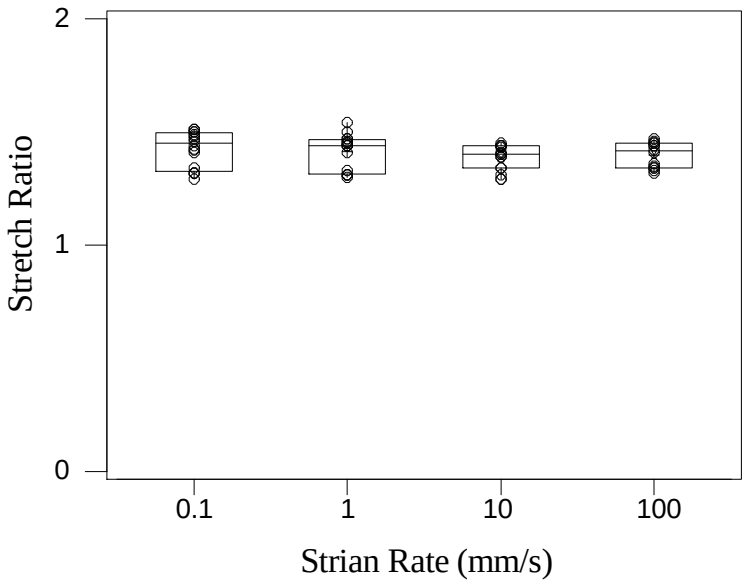

Figure 10. Boxplot of ultimate strain under different loading rates

Creep tests

A second major characteristic of biological soft tissues is their creep response to sustained loads. Since the material is also visco-elastic, a distinction between reversible visco-elastic deformation with time is often confused with creep from permanent damage. Reversible visco-elastic damage is characterized by a return to the original state after sufficient relation. This time scale is typically 5-10 seconds for arterial specimens. The creep studies here reflect more significant damage with to irreversible breakage over minutes to days.

Twenty two ring samples (Table 3) from three different arteries were tested. A lever test system showed as figure 11 was set up. The tests last from few seconds to twenty four hours. All the samples were immersed in a chamber during the tests to prevent desiccation. The displacement versus time curve of representative specimens is shown in Figure 12. Note that the initial deformation during the first 5 seconds is elastic whereas the slope of the displacement after 10 seconds is taken as damage creep since the material is continuously deforming with a constant load.

Table 3: Sample size (N), initial cross-sectional area (A_i), Length (L_i), inner diameter (D_i) and wall thickness (H_i) for SaluBridge and porcine carotid arteries.

Material	N	A_i(mm^2)	L_i (mm)	D_i(mm)	H_i(mm)
Artery 1	4	2.96 (0.20)	3.74 (0.11)	3.82 (0.10)	0.79 (0.04)
Artery 2	5	2.99 (0.41)	3.59 (0.43)	3.84 (0.30)	0.83 (0.04)
Artery 3	5	2.91 (0.29)	3.77 (0.44)	3.48 (0.11)	0.78 (0.05)
Artery 4	8	5.02 (0.39)	4.69 (0.29)	2.45 (0.12)	1.07 (0.04)

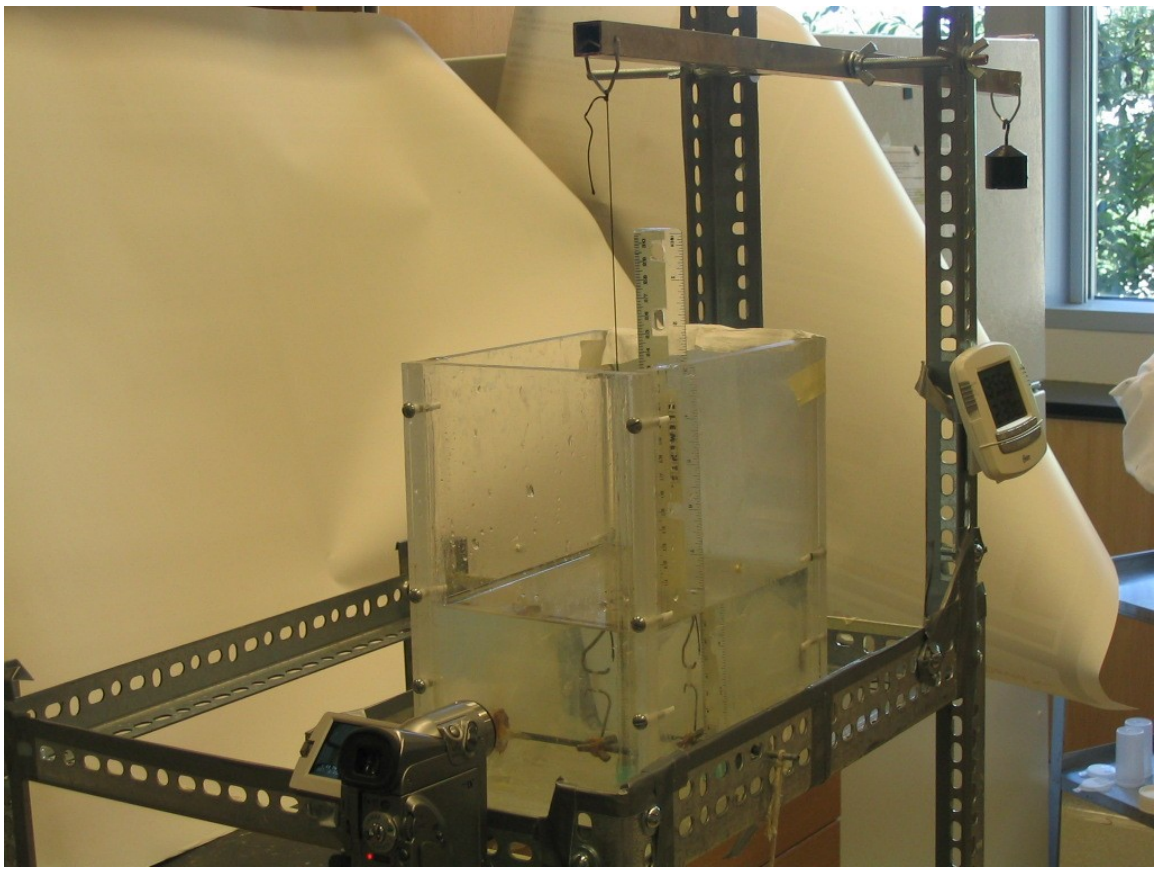

Figure 11. Lever Test System

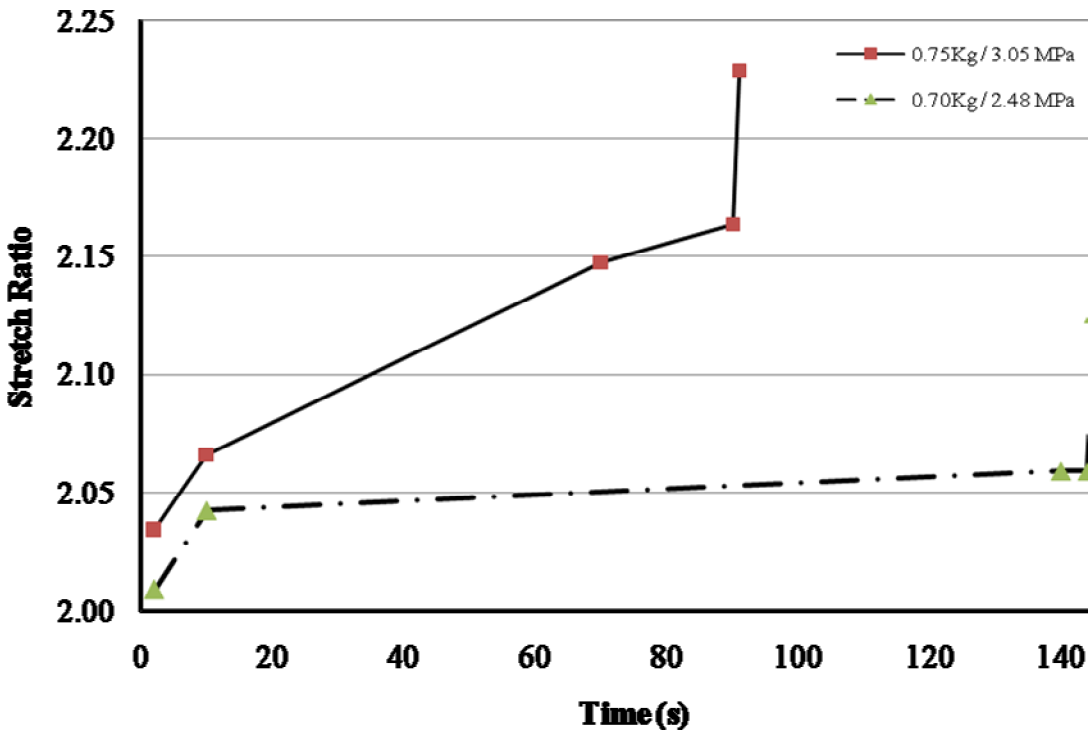

Figure 12. Representative Displacement-Time Curve of Creep Tests

The creep damage ultimately leads to ultimate failure and breakage of the specimen. The stress necessary to induce this failure is a function of the time at load. This relationship is shown in Figure 13 and Figure 14 which shows the ultimate stress vs duration of applied load shown on a log-log plot. This curve in Figure 14 is reminiscent of a typical S-N curve-a power relationship. Note that the exponent of -0.06 is similar as those seen for metals, -0.085 (Julie [44]). The soft tissue tissue's smaller exponent suggests that it is relatively creep resistant in comparison with metals. Nonetheless, the creep curves provides evidence that soft-tissue can accumulate damage at certain stress levels, but is basically elastic, or exhibits no fracture damage, for stress levels below 2.2 MPa.

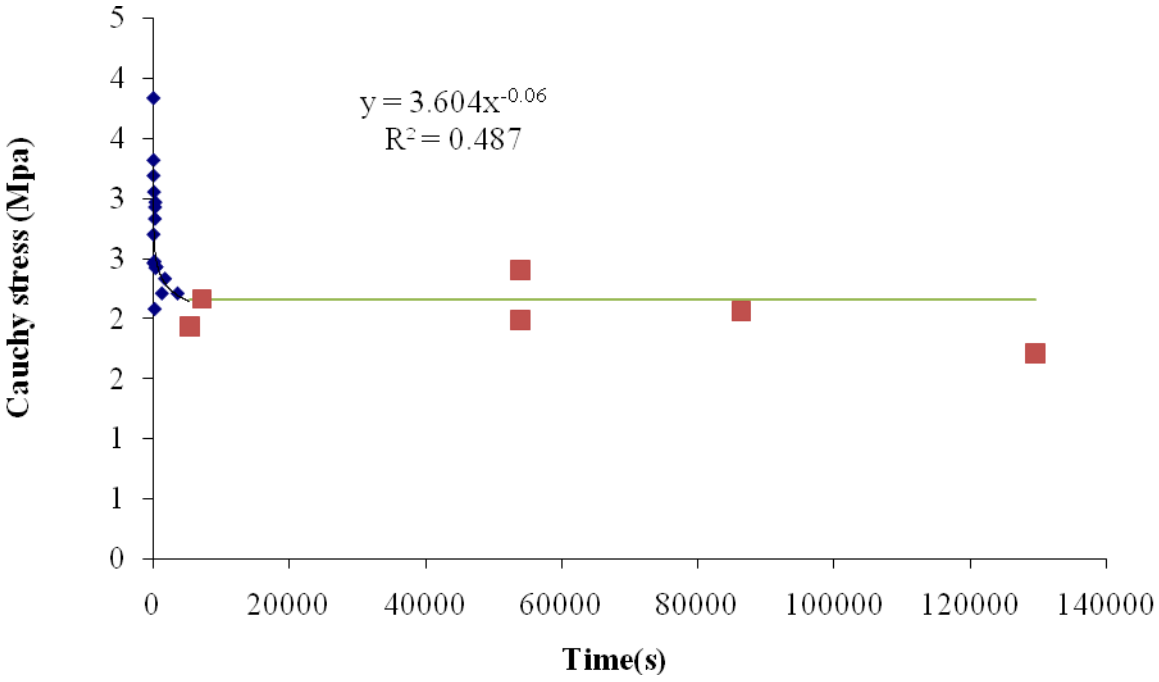

Figure 13. Stress-Time Curve of Creep Tests

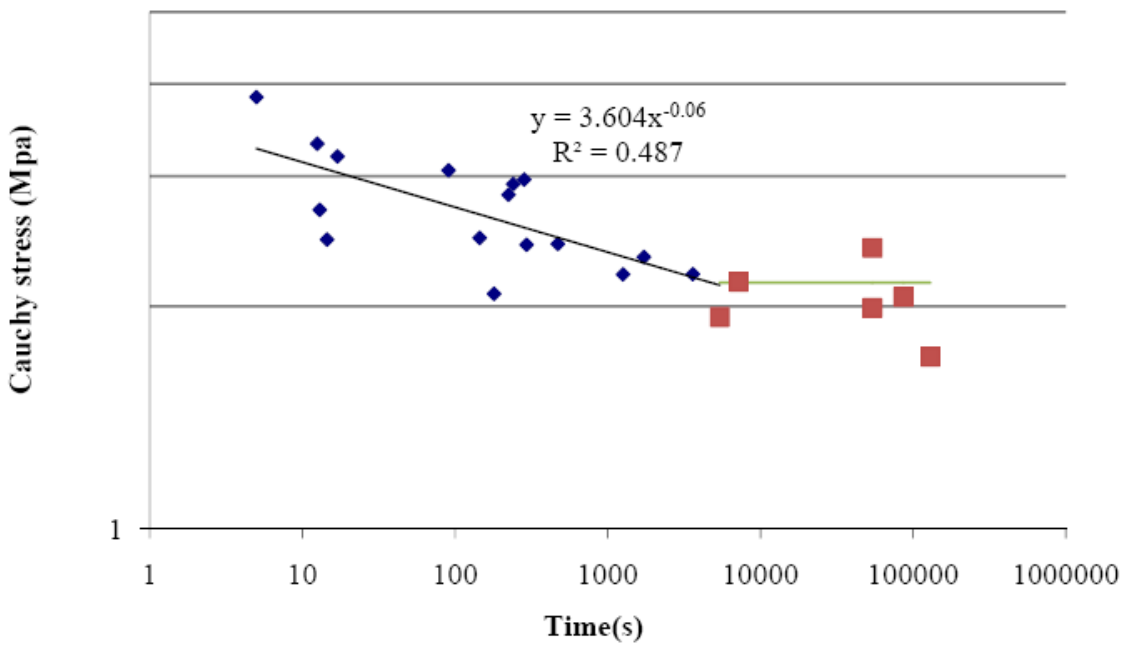

Figure 14. Stress-Time Curve of Creep Tests (Log-Log Scale)

When the logarithm of ultimate stress was plotted against the logarithm of the creep time to failure, a linear correlation can be calculated for plot as Y=K*x+C, which is shown on Figure 15, where y is the ultimate stress, K is the logarithm slope and is negative, and C is a constant. K is negative that means that increases the creep load will shorten the creep time and decreased loads will increase the creep time.

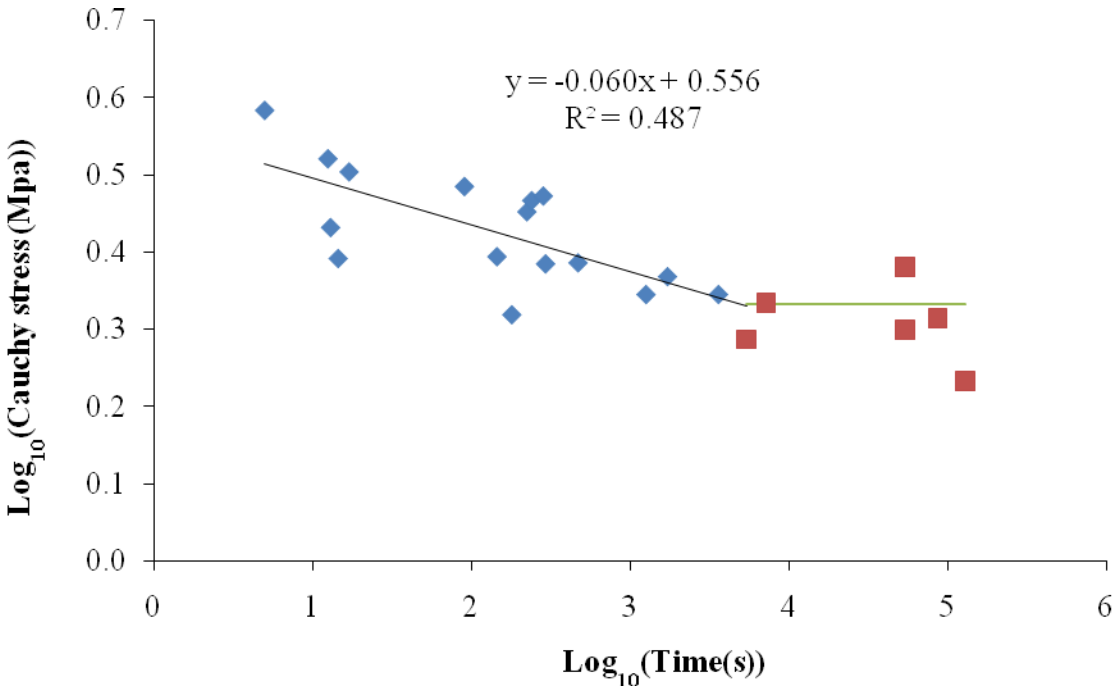

Figure 15. Log Stress-Time Curve of Creep

Cyclic Tests

Arteries are subjected to pulsatile pressures in vivo, not static loads. The ultimate strength of these soft tissues may be strongly influenced by the dynamic loading conditions over static testing. An effort was made to demonstrate the sensitivity of arterial mechanics to cyclic versus static loading. A major limitation is that long term testing was difficult for these harvested biological specimens which deteriorated after a few days at room temperature.

Four pairs of artery specimens were pulled without cycling and with cycling (Table 4). Preconditioning (30% of ultimate stretch, around 2N) was set at 25 cycles to obtain steady state behavior. From each pair one sample was tested directly in tension to failure without cycling to determine the ultimate strength of the artery. The other sample of the pair was cyclically loaded (80% of ultimate stretch, around 3.3N) for 10,000 cycles and then pulled to failure to determine the effect of cycling to ultimate strength.

Table 4: Sample size (N), initial cross-sectional area (A_i), Length (L_i), inner diameter (D_i) and wall thickness (H_i) for SaluBridge and porcine carotid arteries.

Material	N	cycling	A_i(mm^2)	L_i (mm)	D_i(mm)	H_i(mm)
Artery	4	N	4.67 (0.33)	4.25 (0.19)	2.98 (0.05)	1.10 (0.04)
	4	Y	4.82 (0.35)	4.41 (0.29)	3.03 (0.07)	1.09 (0.05)

The cyclic test cycled the sample 10,000 times at 2Hz, and then pulled to failure at a constant strain rate. The Load, Position and Time data from these tests were collected by the computer. The testing data were list in the table 5. It was found that after 10,000 cycling loading, the increase ratio of ultimate force is much more than that of strain, which means that the increase of ultimate force account most of the part of the increase of ultimate stress.

Table 5: Table of cyclic testing data. Samples A1, A3, A6, and B4 without cycling, Samples A2, A5, B1, and B2 with 10,000 cycles.

Sample	A1	A2	A3	A5	A6	B1	B4	B2
Cauchy Stress (MPa)	3.01	3.75	3.23	5.03	3.39	4.43	2.94	3.73
Stetch Ratio	1.44	1.32	1.44	1.22	1.51	1.22	1.37	1.24
Ultimate Force (N)	11.22	11.46	9.58	17.61	10.76	15.20	10.66	12.05
Force / Original Area (N/mm^2)	1.14	1.23	1.13	1.75	1.18	1.48	1.08	1.26
Original Perimeter (mm)	18.40	18.40	18.53	19.47	18.84	19.15	19.15	19.15
Perimeter after Cycling (mm)	22.84	27.06	24.05	31.45	22.86	31.99	26.13	31.23
Perimeter when break (mm)	33.58	35.28	35.83	37.69	36.62	38.19	35.71	37.91

The plots of this data for artery are shown in Figure 16, Figure 17, and Figure 18. The ultimate stress increased after 10,000 cycles, but the ultimate stretch ratio decreased. The values of ultimate strength changed from 3.14±0.21MPa (5233±350 mmHg) without cycling to 4.24±0.62MPa (7066±1033 mmHg) with cycling. The differences of ultimate stress between cycling and no cycling reached statistically significance with p=0.021when we used the Student's paired t-tests method, the level of significance was set at 0.05. At the same time, ultimate strain changed from 1.44±0.06 without cycling to 1.25±0.05 with cycling. The differences of ultimate stress between cycling and no cycling reached statistically significance with p=0.018.

Thus, the arteries repeatedly demonstrated a strengthening phenomenon when subjected to cyclic stretching far beyond the initial 25 cycles of preconditioning.

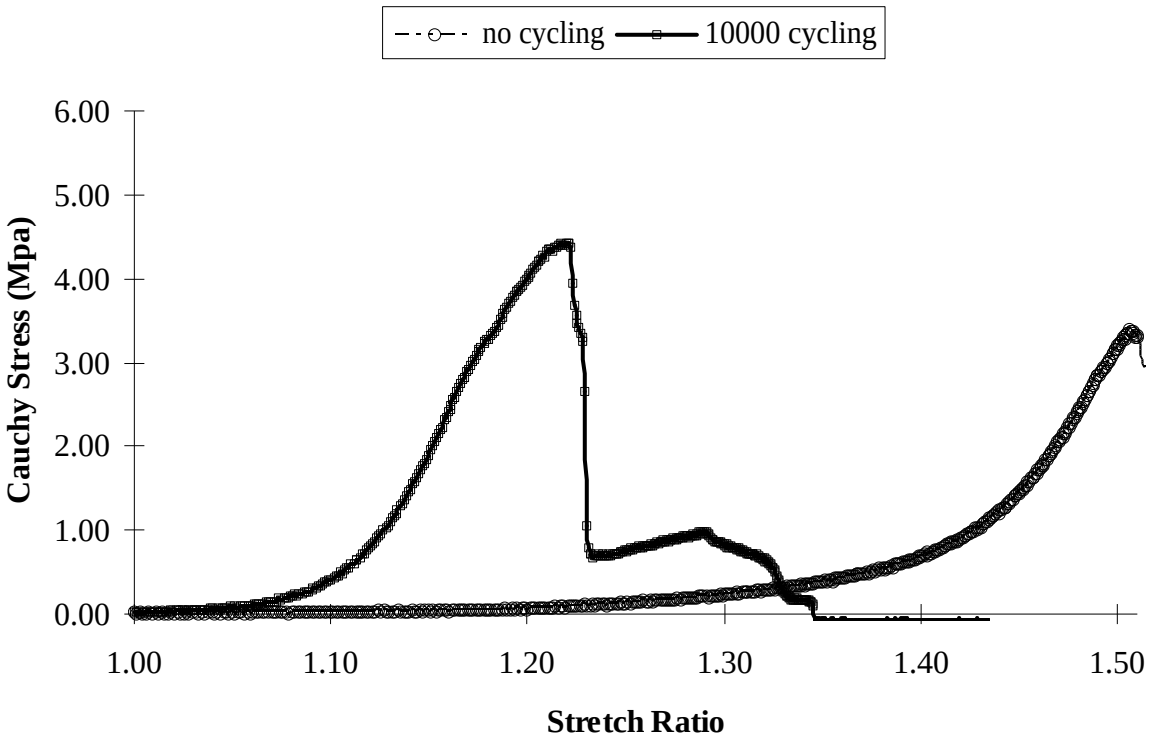

Figure 16. Representative Stress-Strain Response Curve with Cycling and without Cycling

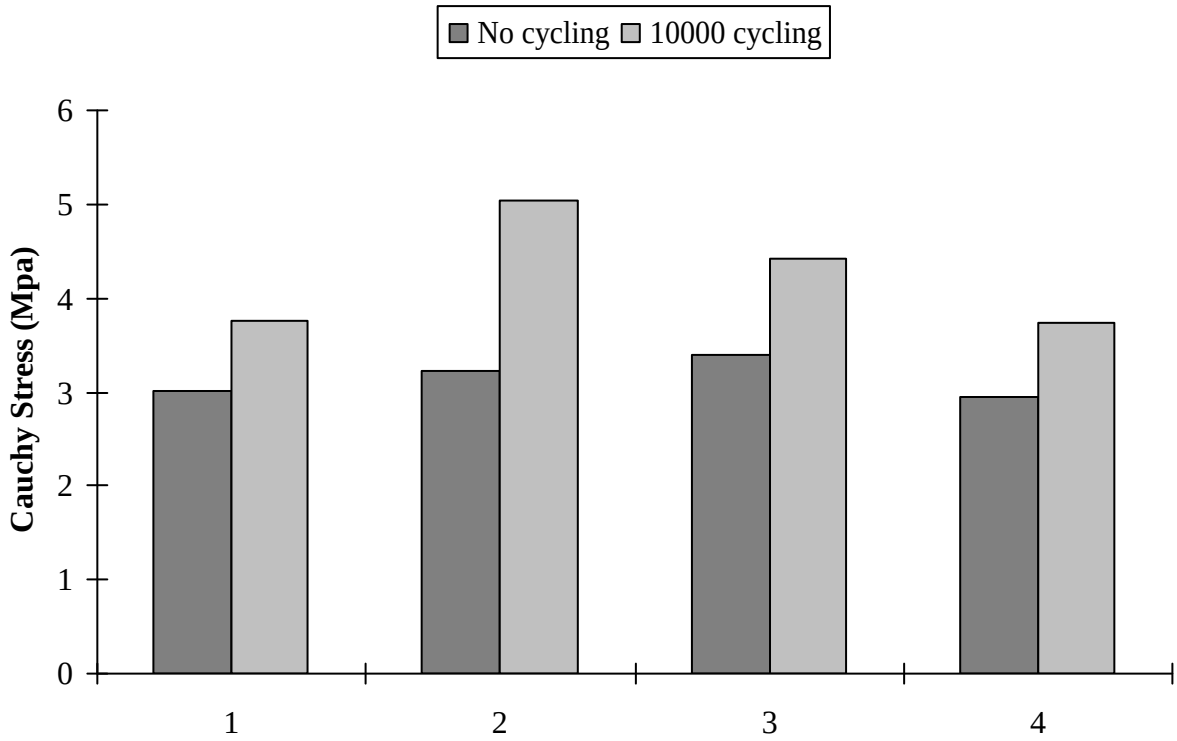

Figure 17. Ultimate Stress with Cycling and without Cycling

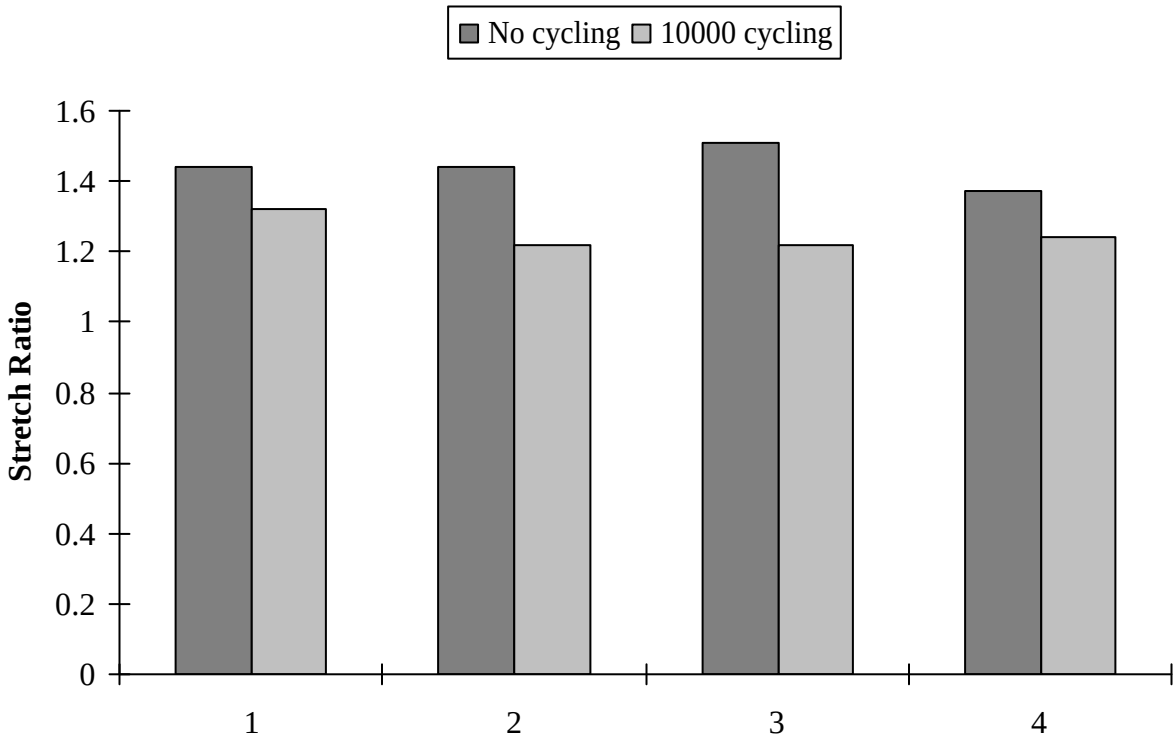

Figure 18. Ultimate Stretch Ratio with Cycling and Without Cycling

Mechanical response of SaluBridge

SaluBridge, created by SaluMedica (Atlanta, GA), may be considered as a potential material for blood vessel substitute. The main components of SaluBridge hydrogel are saline and a highly biocompatible polymer. The specimens, Salubridge-TM, were 5mm in inner diameter and 1mm thick. They were cut into about 4mm sections in a similar fashion as the arteries and Salubridge rings measured in triplicate for an accurate average of length of each ring. They were then transferred to a container and submerged in saline solution until testing to prevent them from dehydrating.

We used the same machine and methods to test Salubia as artery. The samples dimensions are showed in Table 6. The specimens were distracted to ultimate failure at 0.1mm/s and 100mm/s.

Table 6: Sample size (N), initial cross-sectional area (A_i), width (L_i), inner diameter (D_i) and wall thickness (H_i) for SaluBridge and porcine carotid arteries.

Material	N	Speed (mm/s)	A_i(mm^2)	L_i (mm)	D_i(mm)	H_i(mm)
SaluBridge	12	0.1	4.25 (0.45)	4.25 (0.38)	5.00 (0.05)	1.00 (0.04)
	12	100	4.05 (0.41)	4.10 (0.40)	5.00 (0.03)	0.99 (0.05)
Artery	16	0.1	4.39 (0.49)	4.50 (0.25)	3.61 (0.40)	0.97 (0.08)
	16	100	4.07 (0.58)	4.32 (0.30)	3.59 (0.42)	0.94 (0.10)

Knowledge of the mechanical properties of blood vessels is fundamental to understanding the blood vessel graft. Comparing experimental results of mechanical response of blood vessels and SaluBridge to physiologic loads will improve the research of medical therapy or surgical intervention.

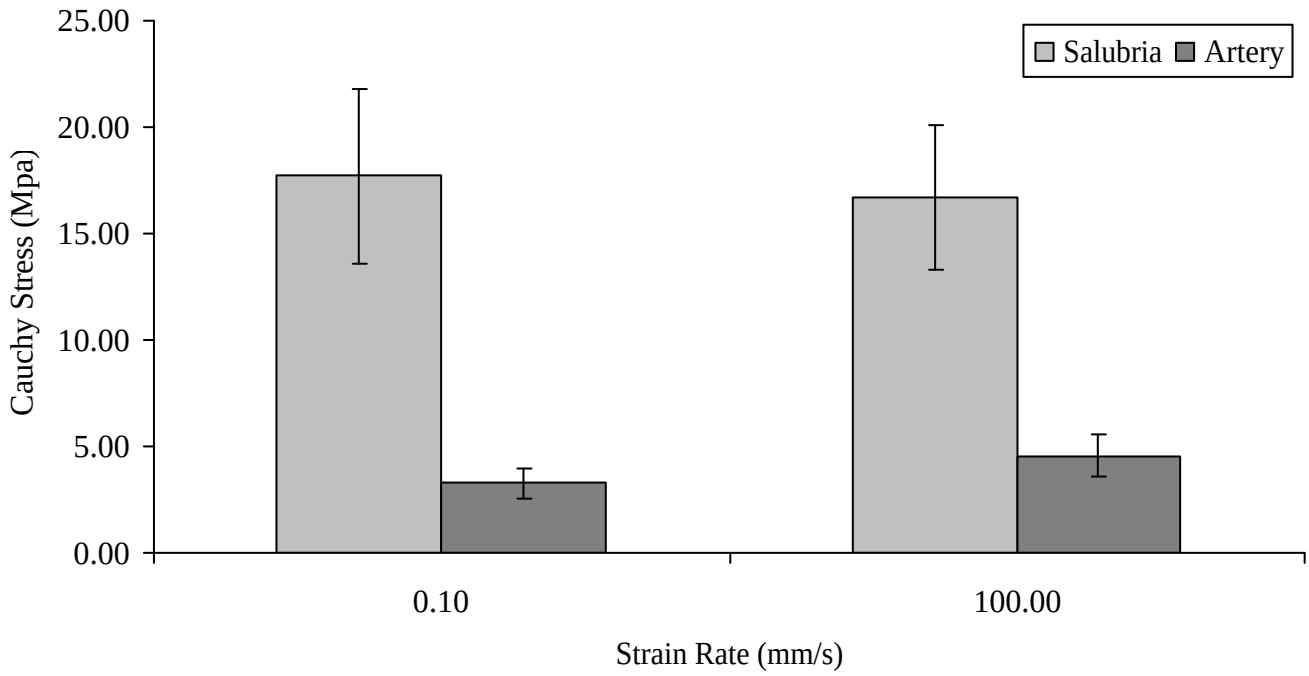

Figure 19. Ultimate Stress (Cauchy) of SaluBridge and Artery

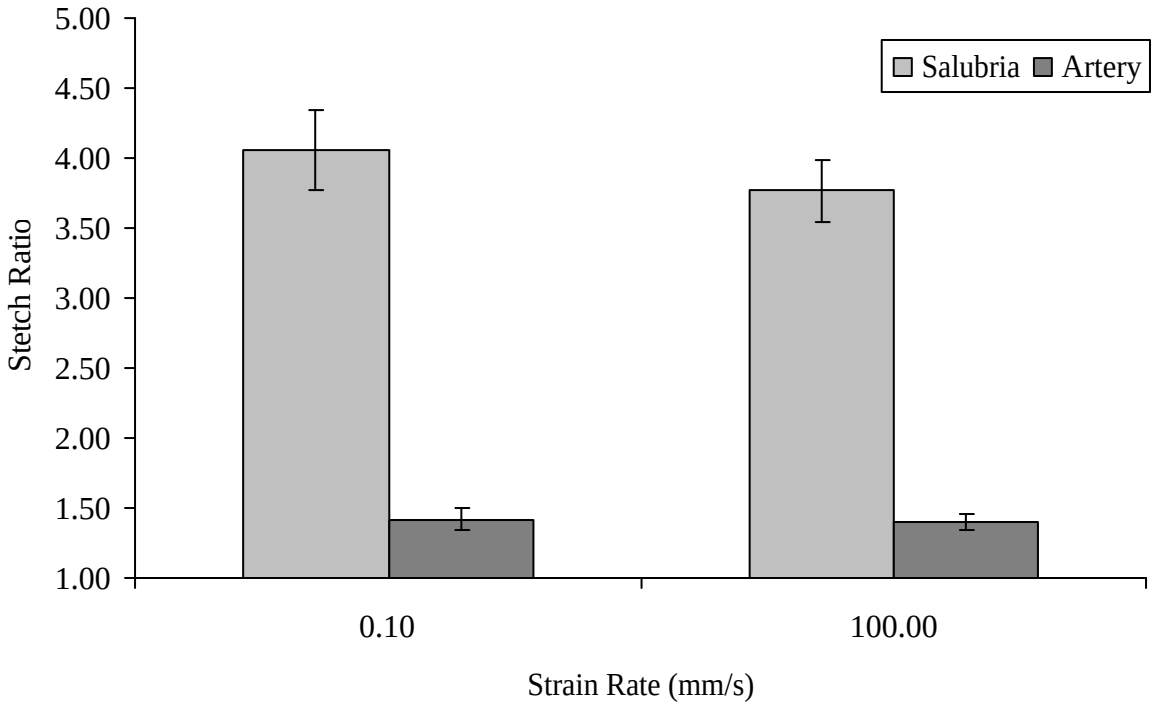

Figure 20. Ultimate Stretch Ratio of SaluBridge and Artery

To discover the mechanical properties difference of artery and SaluBridge, we made the pressure-strain curve based on testing data. The pressure range was set at from 0 mmHg to 150 mmHg.

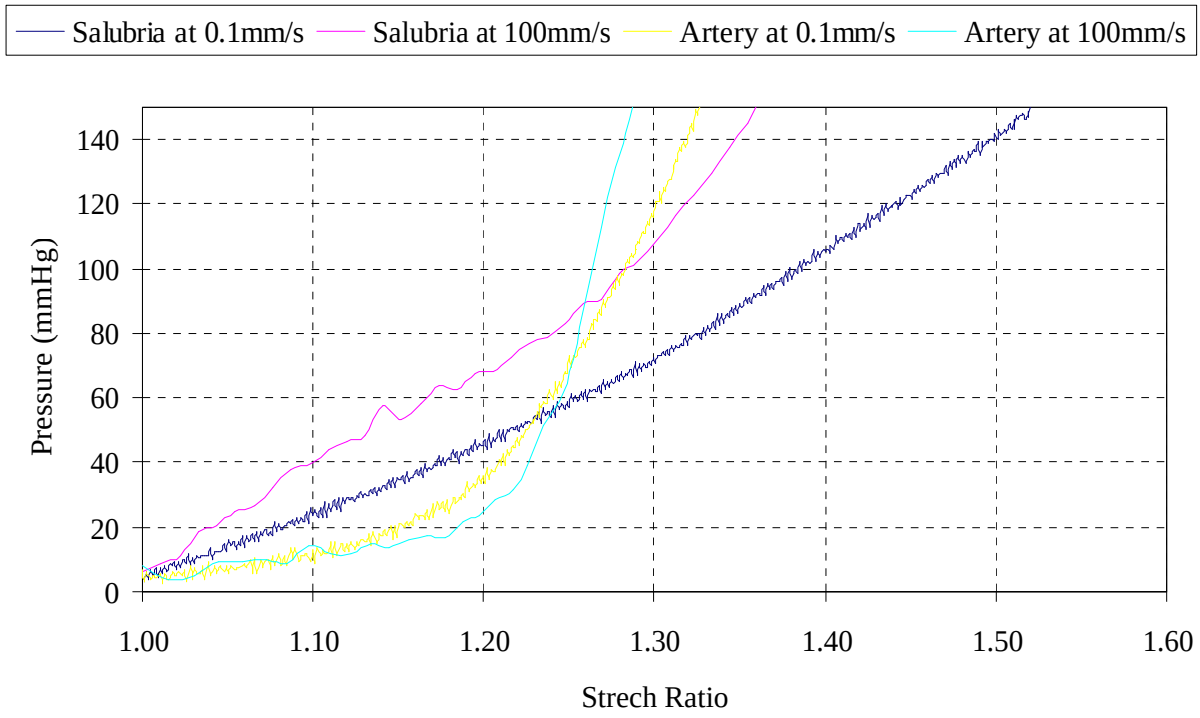

Figure 21. Pressure-Strain curve of SaluBridge and Artery within the Physiological Range of Pressures

Based on the pressure-strain curve, we found that the artery pressure response is more exponential, but the pressure-strain curve for SaluBridge is more linear. We calculated the tangent and secant moduli of artery and SaluBridge which are showed as Table 7. It showed that 60mm Hg to 100mm Hg is the critical region. At this critical region, artery's moduli changed much more than SaluBridge at different strain rates; artery's moduli are about three to five times of SaluBridge's. Thus, SaluBridge is more compliant than porcine carotid arteries, which is also showed in table 8, yet have greater Ultimate Strength and Ultimate Stretch. A stiffer version of SaluBridge has potential as an arterial graft to be compliant matching and be strong enough, something that has eluded previous grafts. Extensive graft related study has been done by William[45], Ku[22], and Rachev[46].

Table 7: Tangent and Secant Moduli Table of artery and SaluBridge

(MPa)	Artery at 0.1mm/s	Artery at 100mm/s	SaluBridge at 0.1mm/s	SaluBridge at 100mm/s
Tangent moduli at 60 mmHg	0.096	0.175	0.036	0.036
Tangent moduli at 80 mmHg	0.115	0.188	0.041	0.048
Tangent moduli at 100 mmHg	0.135	0.265	0.045	0.069
Secant Moduli from 60 to 100 mm Hg	0.128	0.239	0.038	0.036

Table 8: Comparison of Compliance Values [47]

Item	ΔP(mmHg)	$\%\frac{\Delta D}{D_i}$	$\frac{\Delta D}{D_i \Delta P}$ (MPa^{-1})	Investigators
Human Carotid Arteries	80-120	14.7	27.56	Arndt
Saphemous Vein	80-120	1.96	3.68	Sawyer
PTFE	80-120	0.64	1.20	Sawyer
DACRON	80-120	0.76	1.43	Sawyer
SaluBridge (0.1mm/s)	80-120	36	67.51	Fan
SaluBridge (100mm/s)	80-120	34	63.76	Fan

Storage effects on ultimate strength

Because the effect of ex vivo aging storage is unknown, we studied the effect of storage on failure of porcine common carotid artery (Figure 22 and Figure 23). Paired T-tests with the level of significance was set at 0.05 showed that the ultimate stress and strain had no difference among fresh, one-week old and two-week old artery.

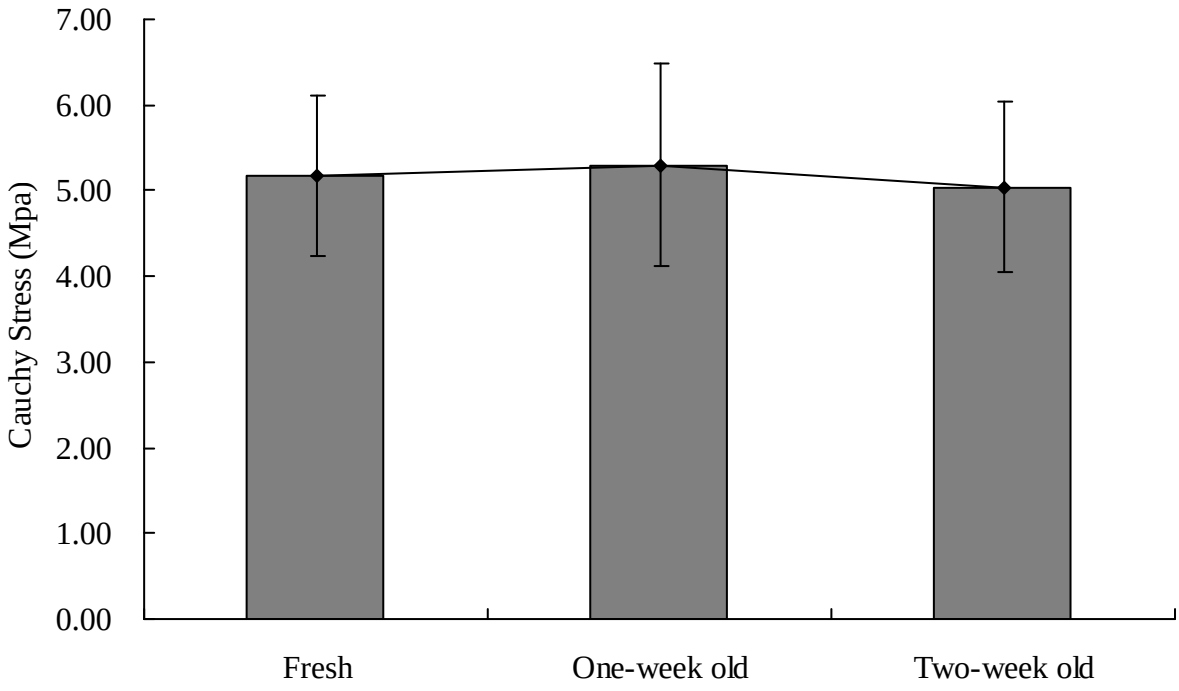

Figure 22. Storage Effects on Ultimate Stress

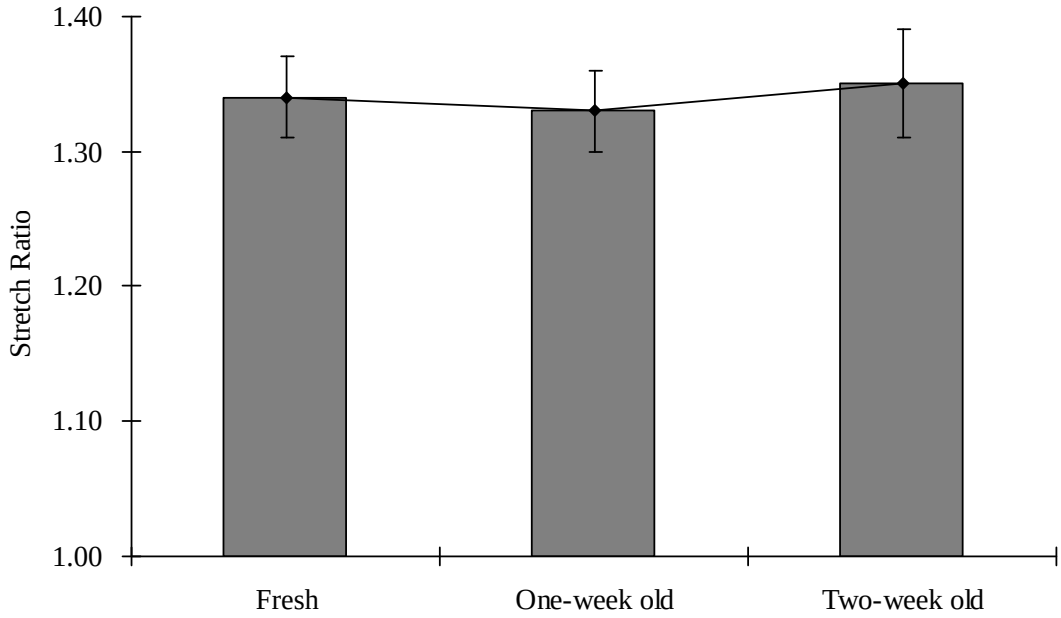

Figure 23. Storage Effects on Ultimate Strain

CHAPTER 4

DISCUSSION

This thesis has quantified some strength properties of porcine coronary arteries. Arteries are cylindrical, anisotropic structures with collagen structural fibers oriented primarily in the circumferential direction. Ring specimens were prepared for ultimate strength determination in tension to avoid gripping problems and crush end-effects. The ultimate strength in tension was approximately 11.46 Newtons in these specimens. A Cauchy stress values were estimated from the specimen cross-section and strain yielding a mean Ultimate Stress of between 3 and 5 MPa, and an Ultimate Strain of between 1.39±0.06 to 1.42±0.08. These values of Ultimate Stress are within the range previously reported. Mohan [18] found that the ultimate stress for human mid-thoracic aortas changed from 1.72±0.89MPa for quasi-static tests to 5.07±3.29MPa for dynamic tests. Raghavan [19] showed that ultimate stress for human abdominal aortic aneurysm (AAA) varied from 0.336MPa to 2.351MPa under a strain rate of 30%/min. Collins [48] showed that the ultimate stress for porcine arteries changed from 3MPa for quasi-static tests to 4-4.5 MPa for dynamic tests (3.5/sec). Monson [49] found that the ultimate stress for human cerebral blood vessels was 4.75±2.18 MPa. The Ultimate Stress of 3 to 5 Mpa can also be converted to a Burst Pressure of 5000 to 8000 mm Hg, which is higher than the burst pressure of porcine arteries of 4200±800 mmHg reported by Chin Quee [43] who used tube specimens.

The Ultimate Strength of the specimens was found to be strain rate dependant. The Ultimate Strength increased by about 39% when the displacement speed was

increased from 0.1 mm/s to 100 mm/s. In contrast, the Ultimate Strain was not sensitive to displacement rate and stayed relatively constant. The dependence of Ultimate Strength on displacement speed is consistent with reports by Mohan who attributed this effect to soft tissues viscoelastic nature.

The study demonstrates that porcine coronary artery ultimate strength increases slightly with increasing strain rates. The increase is approximately 30% over three orders of magnitude of strain rates. Others have shown an increase of up to 50% for human aorta, but little effect on human cerebral arteries and veins (Stemper[50]; Monson[49]). The increase in strength has been attributed to the lining up of fibers (Lawton[32]), differences in wave propagation (Lowenhielm[51]) and hydraulic stiffening (Haut[52]). It is also possible that structural proteins are entangled, thus act as more of a rigid body distributing loads among many fibers at high strain rates. Further histology results may allow us to differentiate these mechanisms.

The finding of the small dependence of coronary artery strength on strain rate has two major applications. First, plaque fracture is likely to occur from local stress concentrations that are subject to pulsatile pressures and bending stresses. The soft tissues may fail over a lifetime of cyclic loading due to damage accumulation. Cyclic loading of coronary arteries may be tested over a range of frequencies to include accelerated fatigue testing in order to make the experiments more tractable. Cyclic testing between 0.5 Hz to 5 Hz should yield similar strength behavior, but dramatically shorter test times. Secondly, the strain rate dependence may have bearing on motor vehicle trauma and other cases of sudden deceleration leading to closed chest trauma and arterial rupture.

The ultimate strength of 5 MPa for coronary arteries sets an upper boundary for the maximum trauma the coronaries may sustain.

Although the ultimate stress changed lightly with strain rate, the ultimate strain was independent of strain rate. This finding is consistent with others in the field(Mohan[18]). Since the material is strain hardening, the failure point leads to small differences in strain at failure.

It should be noted that there are inconsistent results on the relationship between ultimate strength and strain rate. Some authors showed that the ultimate stress is independent of strain rate (Lee [53]; Monson[31]). The possible explanations for this discrepancy are that some studies have limited sample size and some samples were not fresh artery but unhealthy donors. In contrast, present study used sixty four healthy and fresh porcine carotid artery samples.

There are also some discontinuity between current study and previous studies on the effect of loading rate on ultimate strain. Some studies showed that the ultimate strain decreased with increasing loading rate (Collins[48]; Stemper[50]). A possible explanation for this discrepancy is that they may be lack of statistical analysis.

During testing, we found that the intima broke first. Thus the intiama is the weakest part among the three layers of the artery consistent with the analysis of Holzapfel ([54]), which predicts that the intima will break first under the same deformation as media and adventitia. In the clinical setting, arterial subfailure injuries due to blunt trauma typically initiate on inner vessel layers, and then outwards. These partially damaged arteries have clinical problems, such as arterial dilation, thrombosis and stenosis (Stamper[50]).

Time dependant damage of arteries is somewhat masked by the visco-elastic properties of biological soft tissues. Here, constant loads can cause a visco-elastic relaxation which typically reached a steady-state in about 10 seconds. Higher applied loads leads to irreversible elongation over time called creep. The creep proceeded at a linear rate until near fracture when the creep accelerated. For sub-critical stresses less than the acute Ultimate Stress, creep rate was a function of applied stress. A creep-time curve defined the regime of fracture similar to a Stress-Number of cycles (S-N) curve. One can even convert the creep time to a time at load for a 50% duty cycle at a physiologic 1 Hz (Ku [55]). In these cases a 1000 sec creep time may be equivalent to 2000 cycles with a 50% duty cycle. The exponential creep relationship is then analogous to the S-N curve with the coefficient being related to the Ultimate Stress and the exponent related to the fatigue properties. For the porcine coronary arteries, the Ultimate Strength is less than metals, but the exponent value is similar to that for metals (-0.06 vs -0.085) [44].

The creep tests showed a linear logarithm relationship for this soft tissue. Negative slope means that increase the creep load will short the creep time and decrease the loads will increase the creep time. These phenomena demonstrate there was a damage accumulation given the testing time range. The accumulation of damage shown by creep testing indicates that fatigue damage is accumulating and the negative slope of the time vs. load curve indicates that the material will fail faster when increase the testing loads. Further histology tests may allow us to differentiate these mechanisms. The correlation between the ultimate strength and the creep time to failure allows for an estimation of the critical ultimate strength of this soft tissue. The mechanical damage model and

prediction of artery failure may partly count on these critical points. Therefore, combined with other mechanical properties, the damage of soft tissue may be modeled and predicted.

A cyclic fatigue test was attempted for these arteries, but experimental difficulties proved daunting. A fatigue test of pressurizing the arteries at supra-physiologic loads failed due to control feedback issues with our MTS feedback loop. The system noise was larger than the actuator resolution and the system became unstable. A cyclic mechanical test was attempted on ring specimens. The load cell noise prevented running the test using load control. Displacement cycling was ineffectual in that visco-elastic changes and creep constantly reduced the stress levels. While a cyclic stress test is conceptually easy, the systems available to us did not work for elastic soft tissues with high displacements.

For the cyclic tests, the specimens were distracted with displacement control. The values of ultimate strength showed a 35% increase after 10,000 cycles. The differences of ultimate stress between cycling and no cycling reached statistically significance with $p=0.021$. At the same time, ultimate strain had a 13% decrease after cycling and the difference is in statistically with $p=0.018$. The process of cyclic loading increased the ultimate stress and decreased the ultimate strain of arteries. These results may come from tissue fibers rearrangement (Sipkema[34]).

The strength properties of the coronary arteries were then compared against a compliant synthetic polymer tube proposed as a potential coronary vascular graft. The polymer tube had an Ultimate Strength approximately 4X greater than that of the porcine artery. No strain rate effects or creep was noted within the stress ranges less than the Ultimate Strength of the arteries. Thus, this polymeric graft may have inherent strength

greater than a normal coronary artery and provide sufficient safety against rupture or burst.

The effects of storage on the ultimate strength properties provide justification for using stored specimens for these types of experiments. The use of stored specimens is an important practical necessity, especially for time-consuming cyclic testing. The results showed that there were no significant differences on mechanical parameters among fresh arteries and arteries stored at 5° C for one week and two weeks. Also, there was no change on aorta failure tension by 30 days frozen (Raghavan[9]).Other studies have shown that after the initial freeze, mechanical properties of trabecular bone are unaffected by 100 days of storage (Linde[56]).

The storage effects on ultimate strength show above gave us a time window for reliable tests. Although there were no statistically differences among fresh, one-week old and two-week old artery, it is better to run the test within one week because the diameter of the two-week old artery showed a small increase (from 5% to 15%) compared with the fresh artery.

Limitations

Although we would have liked to use human arteries for testing, these samples are difficult to obtain. Porcine arteries are structurally similar to human arteries and they are easy to obtain. So any work that leads to a greater understanding of the porcine artery behavior will help in understanding the behavior of the human tissues.

The ring samples cut by a razor blade may have caused cuts that were not straight. This may affected measurements and possibly changed the distribution of stress. It is possible that forces applied to the specimen when we took the dimension measurements by hand which may have affected of the accuracy of this work. It is impossible to remove all the connective tissue which potentially increased outer diameter measurements. It also may have affected the loading of the material to break. However, great care was taken as possible as we can to cut the connective tissue, to minimize the force applied on the artery and measurements were averaged to compensate for error.

All the samples were stored in the refrigerator (5° C) before testing. All the testing was performed in a bath of PBS to prevent arteries from drying out. However, the testing temperature (24ºC) rather than body temperature (37ºC) may affect the behavior of the tissue. Current study used the ring sample to test the mechanical properties. However, the blood vessel in the body is more like two dimensional stress strain relationship. It is reasonable to use the tubing specimens.

For the ultimate strength and cyclic tests performed in this work the displacement was controlled rather than the load. It will be more accurate to use load control then displacement control since the pressure takes effect for blood vessels in body are.

Future work

This research has determined a range for the ultimate strength and the trend with the strain rate for porcine arteries. The creep tests showed the trend of artery damage with time dependent loading. The mechanical tests on arteries and SaluBridge demonstrated that a physiology compliant vascular graft can be made of polymers and be sufficiently strong. It is necessarily to investigate other studies, such as fatigue limit and suture retention, before graft in the future.

To further the findings of this work it is suggested that cylindrical arterial samples that are cyclically pressurized be performed on porcine arteries since in vivo conditions are cyclic pressure. The corresponding mechanical properties, such as burst pressure with or without cycling, pressure-strain curve, will establish more robust results.

The cyclic tests showed hardening after 10,000 cycling loading and the creep tests showed the progressive damage inside the arteries. All these phenomena definitely have something to do with material structure. In order to better understand the artery failure it is necessary to use histology to observe the changes in these arteries before, during and after testing.

Since we are interested in human atherosclerotic plaque caps, it is better to mimic in vivo environment. It is suggested that all the experiments be performed in the body temperature (37ºC) because we do not know quantitatively how temperatures affect artery mechanical response. All the tests could be extended to human arteries and if possible atherosclerotic plaque caps.

CHAPTER 5

CONCLUSION

In this work tests were performed to determine the ultimate strength and creep behavior of porcine coronary arteries. The ultimate strength results were in the range of 3 MPa to 5 MPa under the strain rate range of 0.1mm/s to 100mm/s. The results agree with those found in previous work on both human and porcine aortic tissue. The ultimate strain results were in the range of 1.3 to 1.5, which were also similar to others' results.

The creep tests results showed the trend of damage accumulation and give us some basic data to model and predict artery failure. Further histology study will allow us to discover these mechanisms.

The cyclic tests discovered that the cyclic loading increased the ultimate stress and decreased the ultimate strain of porcine arteries. Artery tissue fibers rearrangement may account for these changes which made the harvested arteries weaker without preconditioning.

The strength characterization of SaluBridge under uniaxial loading demonstrates that it is possible make a safe, compliant vascular graft by using biocompatible polymeric materials.

In conclusion, this study indicates that porcine coronary arteries exhibit an ultimate stress of approximately 3 to 5 MPa at an ultimate strain of about 1.3 to 1.5. The ultimate stress is weakly dependent on strain rate and appears to be stable over two weeks of storage. The results justify the use of high frequency accelerated testing of these arteries on specimens that are stored under refrigerated conditions for up to two weeks.

The results suggest that the failure of coronary artery tissue and aneurysms can be modeled and then predicted. It also demonstrates that it may be possible to make strong and compliant vascular graft by using polymeric materials.

REFERENCES

1. Manuals, M. *Heart and Blood Vessel Disorders* Atherosclerosis [cited.
2. Vinay Kumar, R.S.C., Stanley L. Robbins *Basic Pathology*. 6th edition ed. 1997: W.B. Saunders Company.
3. Duguid, J.B., *Thrombosis as a factor in the pathogenesis of coronary atherosclerosis.* The Journal of Pathology and Bacteriology, 1946. **58**(2): p. 207-212.
4. Lee, R.T. and P. Libby, *The Unstable Atheroma.* Arterioscler Thromb Vasc Biol, 1997. **17**(10): p. 1859-1867.
5. Richardson, P.D., *Biomechanics of Plaque Rupture: Progress, Problems, and New Frontiers.* Annals of Biomedical Engineering, 2002. **30**(4): p. 524-536.
6. McCord, B., *Fatigue of Atherosclerotic Plaque,* in *Mechanical Engineering*. 1993, Georgia Institute of Technology: Atlanta,GA.
7. Barger AC, B.R., Lainey LL, Silverman KJ, *Hypothesis: vasa vasorum and neovascularization of human coronary arteries. A possible role in the pathophysiology of atherosclerosis.* N Engl J Med. , 1984. **310**(3): p. 175-177.
8. Leary, T., *Coronary spasm as a possible factor in producing sudden death.* American Heart Journal, 1935. **10**(3): p. 338-344.
9. Richardson, P.D., M.J. Davies, and G.V.R. Born, *INFLUENCE OF PLAQUE CONFIGURATION AND STRESS DISTRIBUTION ON FISSURING OF CORONARY ATHEROSCLEROTIC PLAQUES.* The Lancet, 1989. **334**(8669): p. 941-944.

10. Gertz, S.D. and W.C. Roberts, *Hemodynamic shear force in rupture of coronary arterial atherosclerotic plaques.* The American Journal of Cardiology, 1990. **66**(19): p. 1368-1372.

11. Loree H. M., K.R.D., Atkinson C. M., Lee R. T., *Turbulent pressure fluctuations on surface of model vascular stenoses.* American journal of physiology, 1991. **261**(30): p. H644-H650.

12. Bank, A.J., et al., *Atherosclerotic plaque rupture: a fatigue process?* Medical Hypotheses, 2000. **55**(6): p. 480-484.

13. Versluis, A., A.J. Bank, and W.H. Douglas, *Fatigue and plaque rupture in myocardial infarction.* Journal of Biomechanics, 2006. **39**(2): p. 339-347.

14. Lee, R.T., et al., *Structure-dependent dynamic mechanical behavior of fibrous caps from human atherosclerotic plaques.* Circulation, 1991. **83**(5): p. 1764-1770.

15. Libby, P., *Molecular Bases of the Acute Coronary Syndromes.* Circulation, 1995. **91**(11): p. 2844-2850.

16. Suresh, S., *Fatigue of Metarials*. 1998, Cambridge University Press.

17. Dvorak, G.J.a.J., W.S., *Fatigue of Metal Matrix Composites.* International Journal of Fracture, 1980. **16**(6): p. 585-607.

18. Mohan, D. and J.W. Melvin, *Failure properties of passive human aortic tissue. I--Uniaxial tension tests.* Journal of Biomechanics, 1982. **15**(11): p. 887-893.

19. Raghavan, M.L., et al., *Regional distribution of wall thickness and failure properties of human abdominal aortic aneurysm.* Journal of Biomechanics, 2006. **39**(16): p. 3010-3016.

20. Johnson, G.A., Tramaglini, Dawn M., Levine, Rebecca E., Ohno, Kazunori, Choi, Nam-Yong, Woo, Savio L-Y, *Tensile and Viscoelastic Properties of Human Patellar Tendon.* Journal of Orthopaedic Research, 1993. **12**: p. 796-803.

21. Edwards, C. and R. Marks, *Evaluation of biomechanical properties of human skin.* Clinics in Dermatology, 1995. **13**(4): p. 375-380.

22. Ku, D.N., Meyer, Ralph A., Sarabia, Xavier R., Williams, Stephen N. , *Meniscus prosthesis* 2004, SaluMedica LLC USA.

23. Bergel, D.H., *The static elastic properties of the arterial wall.* The Journal of Physiology, 1961. **156**(3): p. 445-457.

24. Bergel, D.H., *The dynamic elastic properties of the arterial wall.* The Journal of Physiology, 1961. **156**(3): p. 458-469.

25. Dobrin, P.B., *Mechanical properties of arterises.* Physiol. Rev., 1978. **58**(2): p. 397-460.

26. Langewouters, G.J., K.H. Wesseling, and W.J.A. Goedhard, *The static elastic properties of 45 human thoracic and 20 abdominal aortas in vitro and the parameters of a new model.* Journal of Biomechanics, 1984. **17**(6): p. 425-435.

27. Silver FH, C.D., Buntin CM, *Mechanical properties of the aorta: a review.* Crit Rev Biomed Eng., 1989. **17**(4): p. 323-358.

28. Angouras, D., et al., *Effect of impaired vasa vasorum flow on the structure and mechanics of the thoracic aorta: implications for the pathogenesis of aortic dissection.* European Journal of Cardio-Thoracic Surgery, 2000. **17**(4): p. 468-473.

29. Bank, A.J., et al., *Contribution of Collagen, Elastin, and Smooth Muscle to In Vivo Human Brachial Artery Wall Stress and Elastic Modulus.* Circulation, 1996. **94**(12): p. 3263-3270.

30. Fung, Y.C., *Biomechanics-Mechancal Properties of Living Tissues*. 1993: Springer-Verlag.

31. Monson, K.L., et al., *Axial Mechanical Properties of Fresh Human Cerebral Blood Vessels.* Journal of Biomechanical Engineering, 2003. **125**(2): p. 288-294.

32. Lawton, R.W., *Measurements on the Elasticity and Damping of Isolated Aortic Strips of the Dog.* Circ Res, 1955. **3**(4): p. 403-408.

33. Mohan, D., *Failure properties of passive human aortic tissue. II--Biaxial tension tests.* Journal of Biomechanics, 1983. **10**(1): p. 31-44.

34. Sipkema, P., et al., *Effect of cyclic axial stretch of rat arteries on endothelial cytoskeletal morphology and vascular reactivity*. Journal of Biomechanics, 2003. **36**(5): p. 653-659.

35. Han, H.-C., *A biomechanical model of artery buckling.* Journal of Biomechanics. **In Press, Corrected Proof**.

36. SATO, T.M.a.M., *Analysis of Stress and Strain Distribution in the Artery Wall Consisted of Layers with Different Elastic Modulus and Opening Angle.* JSME International Journal. Series C., 2002. **45**(4): p. 906-912.

37. Blondel, W.C.P.M.D., J.; Maurice, G.; Carteaux, J.-P.; Xiong Wang; Stolz, J.-F., *Investigation of 3-D mechanical properties of blood vessels using a new in vitro tests system: results on sheep common carotid arteries.* Biomedical Engineering, IEEE Transactions on, 2001. **48**(4): p. 442-451.

38. Hayashi, K. and Y. Imai, *Tensile property of atheromatous plaque and an analysis of stress in atherosclerotic wall.* Journal of Biomechanics, 1997. **30**(6): p. 573-579.

39. Tang, D., et al., *Local Maximal Stress Hypothesis and Computational Plaque Vulnerability Index for Atherosclerotic Plaque Assessment.* Annals of Biomedical Engineering, 2005. **33**(12): p. 1789-1801.

40. Tang, D., et al., *Generalized finite difference method for 3-D viscous flow in stenotic tubes with large wall deformation and collapse.* Applied Numerical Mathematics, 2001. **38**(1-2): p. 49-68.

41. Wootton, D., et al., *A Mechanistic Model of Acute Platelet Accumulation in Thrombogenic Stenoses.* Annals of Biomedical Engineering, 2001. **29**(4): p. 321-329.

42. Lally, C., Reid, A.J., and Pendergast, P.J., *Elastic Behavior of Porcine Artery Tissue under Uniaxial and Equibiaxial Tension.* Annals of Biomedical Engineering, 2004. **32**(10): p. 1355-1364.

43. Chin Quee, S.L.H., *Design Verification for Tissue Engineered Vascular Grafts*, in *Mechanical Engineering*. 2001, Georgia Institute of Tehcnology: Atlanta, GA.

44. Julie A. Bannantine, J.J.C., James L. Handrock *Fundamentals of Metal Fatigue Analysis*. 1989: Prentice Hall.

45. Williams, S., *Mechanical Testing of Biomaterials for Potential Use as a Vascular Graft and Auricular Cartilage Replacement*, in *Mechanical Engineering*. 1998, Georgia Institute of Technology: Atlanta.

46. Alexander Rachev, L.F., David Ku, *Design and Fabrication of Mechanics-matching Arterial Grafts,* in *2005 Summer Bioengineering Conference*. 2005: Colorado.

47. R. Roeder, J.W.N.L.T.H.L.A.G.J.O., *Compliance, elastic modulus, and burst pressure of small-intestine submucosa (SIS), small-diameter vascular grafts.* Journal of Biomedical Materials Research, 1999. **47**(1): p. 65-70.

48. Collins, R. and W.C.L. Hu, *Dynamic deformation experiments on aortic tissue.* Journal of Biomechanics, 1972. **5**(4): p. 333-334.

49. Monson, K.L., et al., *Significance of source and size in the mechanical response of human cerebral blood vessels.* Journal of Biomechanics, 2005. **38**(4): p. 737-744.

50. Stemper, B.D., N. Yoganandan, and F.A. Pintar, *Mechanics of arterial subfailure with increasing loading rate.* Journal of Biomechanics. **In Press, Corrected Proof**.

51. Lowenhielm, P., *Dynamic properties of the parasagittal bridging veins.* Zeitschrift fur Rechtsmedizin, 1974. **74**(1): p. 55-62.

52. Haut, T.L. and R.C. Haut, *The state of tissue hydration determines the strain-rate-sensitive stiffness of human patellar tendon.* Journal of Biomechanics, 1997. **30**(1): p. 79-81.

53. Lee, M.-C. and R.C. Haut, *Insensitivity of tensile failure properties of human bridging veins to strain rate: Implications in biomechanics of subdural hematoma.* Journal of Biomechanics, 1989. **22**(6-7): p. 537-542.

54. Holzapfel, G.A., et al., *Determination of layer-specific mechanical properties of human coronary arteries with nonatherosclerotic intimal thickening and related constitutive modeling.* Am J Physiol Heart Circ Physiol, 2005. **289**(5): p. H2048-2058.

55. David N. Ku, P.R.G., *Scleral Creep in Vitro Resulting from Cyclic Presure Pulses: Applications to Myopia.* Am J of Opt & Physiol Optics, 1981. **58**(7): p. 528-535.

56. Linde, F. and H.C.F. Sorensen, *The effect of different storage methods on the mechanical properties of trabecular bone.* Journal of Biomechanics, 1993. **26**(10): p. 1249-1252.